

A new phoronid species, *Phoronis embryolabi*, with a novel type of development, and consideration of phoronid taxonomy and DNA barcoding

Elena N. Temereva^{A,D} and Anton Chichvarkhin^{B,C}

^A119991, Russia, Moscow, Vorobiev Gory 1-12, Moscow State University, Biological Faculty, Dept. Invertebrate Zoology.

^B690041, Russia, Vladivostok, Palchevskogo st., 17, National Science Center of Marine Biology, Far Eastern Branch of Russian Academy of Sciences.

^C690950, Russia, Vladivostok, Suhanova st., 8, Far Eastern Federal University.

^DCorresponding author. Email: temereva@mail.ru

Abstract. The Phoronida, which is one of the smallest phyla of invertebrates, includes only 13 valid species, although ~40 larval forms of phoronids were recently described. This report uses light microscopy and molecular methods to describe a new phoronid species, *Phoronis embryolabi* Temereva & Chichvarkhin, sp. nov. The morphology of *P. embryolabi*, which lives commensally in the burrows of Axiidea shrimp *Nihonotrypaea japonica* in Vostok Bay (the Sea of Japan), is extremely similar to that of *Phoronis pallida* Silen, 1952; the bodies of both species exhibit specific regionalisation. However, the organisation of the metanephridia differs between *P. pallida* and *P. embryolabi*. Moreover, *P. embryolabi* has a unique type of development, viviparity, in which mothers release fully developed larvae into the environment. In all other phoronid species, the spawning occurs as a release of fertilised eggs or early embryos. Viviparity of completely developed larvae has not been previously described for any phoronid. According to analysis of partial 28S rRNA, *P. embryolabi* is close to *Phoronis pallida*. On the other hand, analysis of partial cytochrome *c* oxidase subunit I indicated a unique position of *P. embryolabi* among phoronids. These results should be used for revision of phoronid taxonomy (i.e. the type of development should be considered as characteristic of subgenera within the genus *Phoronis*). This report also establishes the relationship between *P. embryolabi* and an *Actinotrocha* sp. that was described in a previous paper.

Additional keywords: 28S rRNA, actinotroch, *COI*, cytochrome *c* oxidase subunit 1, morphology, Phoronida.

Received 3 April 2016, accepted 15 August 2016, published online 16 March 2017

Introduction

Phoronids are marine invertebrates with a biphasic life cycle. There are 13 accepted phoronid species, most of which have a worldwide distribution (Temereva and Malakhov 1999; Temereva 2000; Hirose *et al.* 2014). Adult benthic phoronids live in a tube that is produced by the epidermal glands. These tubes are embedded in soft sediment or are attached to hard substrata. Based on this difference, phoronids are divided into two ecological groups: dwelling phoronids living in the rocks, shells of molluscs and shelters of cirripedians and soft-sediment-living phoronids. However, there are some phoronids that inhabit both environments (e.g. *Phoronis hippocrepia*) (Emig 1982). In the latter case, the tube is agglutinated by particles of sand or mud. Adult phoronids live as commensals of invertebrates: bivalves, gastropods, cirripedians, sponges and cnidarians (Temereva 2009). Identification of adult phoronids is extremely difficult because morphology varies greatly within

species and because identification requires the preparation of several series of histological sections (Emig 1979).

Although morphology has been successfully used to determine differences between some species of the Phoronida (Silén 1952; Emig 1979; Temereva 2000), other species are difficult to distinguish using traditional morphological approaches (Temereva and Malakhov 1999; Hirose *et al.* 2014). This is especially true for immatures stages and for heavily damaged specimens. Overcoming this problem requires the development of an accurate and high-throughput approach that does not depend on morphology, and DNA barcoding is such an approach (Sin *et al.* 2009; Undheim *et al.* 2010). DNA barcoding can help researchers assign individuals to known species when morphological characters are missing or misleading (Schindel and Miller 2005). Over the past decade, DNA barcoding, which is usually based on the nucleotide sequence of one short DNA fragment, has been used to quickly and reliably

identify known species and to aid in the discovery of cryptic species (Hebert *et al.* 2003, 2004a, 2004b; Ward *et al.* 2005; Barr *et al.* 2009; Chen *et al.* 2011). The use of a standardised fragment of cytochrome *c* oxidase subunit I (*COI*) in the mitochondrial DNA (mtDNA) was first advocated by Hebert *et al.* (2003). Substantial evidence indicates that *COI* sequences (e.g. the DNA barcodes) can be used to identify both terrestrial and aquatic taxa (e.g. Hebert *et al.* 2004a, 2004b; Ward *et al.* 2005; Clare *et al.* 2007; Feng *et al.* 2011; Turanov and Kartavtsev 2014). The efficacy of *COI*-based barcoding in the discovery of cryptic species has also been documented for several taxa (e.g. Hebert *et al.* 2004a; Hebert and Gregory 2005; Chen *et al.* 2011).

Despite the broad benefits of DNA barcoding, several problems arise when it is used alone for species delimitation (e.g. Hebert *et al.* 2004a; Hebert and Gregory 2005; Chen *et al.* 2011). These shortcomings include: misidentification of voucher specimens (Will and Rubinoff 2004; Becker *et al.* 2011); confusion of the terms ‘species identification’, ‘species delimitation’ and ‘species discovery’ (DeSalle *et al.* 2005; Brower 2006; DeSalle 2006; Goldstein and DeSalle 2011); inappropriate use of neighbour-joining (NJ) trees (Will and Rubinoff 2004; Meier *et al.* 2006; Meier 2008; Goldstein and DeSalle 2011) and bootstrap resampling values (Lowenstein *et al.* 2010; Collins *et al.* 2012; Zhang *et al.* 2012); misinterpretation of the barcoding gap (Wiemers and Fiedler 2007; Collins and Cruickshank 2012); incorrect use of fixed-distance thresholds (Zhang *et al.* 2012); use of corrected (i.e. biased) distances (Srivathsan and Meier 2012); and the conflation of tested hypotheses (Meier 2008; Goldstein and DeSalle 2011). These shortcomings are apparently avoided by several recently developed methodological approaches (e.g. Meier *et al.* 2006; Pons *et al.* 2006; Sarkar *et al.* 2008; Puillandre *et al.* 2012).

To date, *COI* and *28S* markers have been sequenced for a range of phoronid species (Santagata and Cohen 2009). These markers have been useful for identifying species and for highlighting potentially overlooked species (e.g. Undheim *et al.* 2010; Allcock *et al.* 2011; Ekimova *et al.* 2015). *COI* and *28S* have also been used to study the phylogeny of phoronids at the infraspecific level (Santagata and Cohen 2009).

All phoronids have external–internal fertilisation: spermatozooids are released from spermatophores, penetrate into the female and fertilise oocytes in the trunk coelom (Ikeda 1903; Zimmer 1964; Emig 1982; Temereva and Malakhov 2006, 2012). The cleavage is triggered by fertilised eggs coming into contact with water after spawning (Zimmer 1964). In some phoronid species (i.e. *Phoronopsis harmeri*) the cleavage of eggs occurs in the maternal trunk and the two- and four-cell embryos are found in the trunk coelom and nephridial canals (Selys-Longchamps 1907; Rattenbury 1953; Forneris 1959; Emig 1977; Temereva and Malakhov 2007, 2012). Three types of development have been described for phoronids: holopelagy, brooding and lecithotrophy (Emig 1977; Temereva and Malakhov 2012). In phoronids with holopelagic development, all stages of development from egg to competent larvae occur in water. Phoronids brood embryos until they become larvae in embryonic masses between the tentacles. One phoronid species has lecithotrophic development; its embryos and larvae develop in the mother’s tube. Regardless of type of development, all

phoronids spawn fertilised eggs or early embryos. In this report, we describe a new phoronid species that has an unusual type of development, viviparity, in which the mother gives birth to fully developed larvae.

Materials and methods

Sampling of animals and light microscopy

Adult phoronids and larvae were collected in July 2015 in Vostok Bay, Sea of Japan. Adult phoronids with sediment were removed from the burrows of the shrimp *Nihonotrypaea japonica* with a vacuum pump. The pump was driven into the burrow holes, which are located at a depth of 60 m. Tubes with animals were separated from sediment by washing through a sieve with 2-mm openings. The tubes were collected in sea water, and the live animals were photographed with a digital camera mounted on a Leica MZ12.5 stereomicroscope. Larvae were collected with a deep net (a net with long handle and gauze), observed with an Olympus XI83 microscope, photographed and fixed in 96% ethanol for molecular study. The specimens used for molecular analysis are listed in Table 1.

For light microscopy, tubes with animals inside were fixed whole, without dissection, at 4°C in 2.5% glutaraldehyde in 0.05 M cacodylate buffer containing NaCl, and were then post-fixed in 1% osmium tetroxide in the same buffer. The specimens were dehydrated in ethanol followed by an acetone series and were then embedded in EMBed-812. Semi-thin sections were cut with a Leica UC6 ultramicrotome (Leica Microsystems GmbH, Wetzlar, Germany). Semi-thin sections were stained with methylene blue, observed with a Zeiss Axioplan2 microscope, and photographed with an AxioCam HRm camera (Carl Zeiss, Oberkochen, Germany). Three-dimensional models were constructed using 3D-Doctor software (Able Software Corp).

DNA extraction, PCR and sequencing

For DNA amplification and sequencing, parts of live adult animals were extracted from the tube, fixed in 96% ethanol and kept at –20°C.

Genomic DNA was extracted from 50 mg of preserved tissue using a DNeasy extraction kit (Qiagen, Valencia, CA, USA) according to the manufacturer’s protocol. The DNA elutant was preserved at –20°C. DNA extracts of the new species (*Phoronis embryolabi*, see ‘Results’) were obtained on three separate occasions using tissue from individual adults and larvae.

DNA amplification and sequencing

PCR was used to amplify two molecular markers, *COI* and *28S*, which correspond to the portions of the mitochondrial cytochrome *c* oxidase subunit 1, and nuclear *28S* rRNA genes, respectively. *COI* was amplified with primers LCO1490 5'-GGT CAA CAA ATC ATA AAG ATA TTG G-3', HCO2198 5'-TAA ACT TCA GGG TGA CCA AAA AAT CA-3', which were developed by Folmer *et al.* (1994). The *28S* rRNA was amplified in two parts with primers 28S-C1 5'-ACC CGC TGA ATT TAA GCA T-3', 28S-C2rev 5'-ACT CTC TCT TCA AAG TTC TTT TC-3' and 28S-C2 5'-GAA AAG AAC TTT GAA GAG AGA GT-3', LSU_rev1 5'-TACTA

Table 1. List of sequenced samples and National Centre of Biotechnology Information (NCBI) accession numbers for nucleotide sequences

Species	Voucher #	Location	NCBI accession number	
			<i>COI</i>	Species 28S
<i>Phoronis embryolabi</i>	18-1 (adult)	Vostok Bay, Sea of Japan	A	A
<i>Phoronis embryolabi</i>	18-2 (larva)	Vostok Bay, Sea of Japan	A	A
<i>Phoronis ijimai</i>	17-1	Avacha Bay, Bering Sea	A	A
<i>Phoronis ijimai</i>	18-3	Vostok Bay, Sea of Japan	A	A
<i>Phoronis vancouverensis</i>			EU484462	n/a
<i>Phoronis pallida</i>			n/a	EU334116
<i>Phoronis australis</i> 1			EU484458	EU334111
<i>Phoronis australis</i> 2			EU484457	EU334110
<i>Phoronis emigi</i>			AB621915	AB621914
<i>Phoronis psammophila</i>			AY368231	n/a
<i>Phoronis californica</i>			EU484463	EU334118
<i>Phoronis ovalis</i>			EU484461	EU334115
<i>Phoronis architecta</i>			n/a	EU334109
<i>Phoronis hippocrepia</i>			EU484459	AY839251
<i>Phoronis muelleri</i>			EU484460	EU334114
<i>Phoronopsis harmeri</i>	18-10	Vladivostok, Sea of Japan	A	A
<i>Phoronopsis viridis</i>			EU484465	AY428825
<i>Plagioecia patina</i>			FJ196102	FJ409597
<i>Laqueus californianus</i>			AB026503	AY210460

^AFor the accession numbers, please refer to Table S1 (available as Supplementary material). Data were obtained in this study.

GAAGGTTTCGATTAGTC-3', which were developed by Gouÿ de Bellocq *et al.* (2001) and Sonnenberg *et al.* (2007) respectively. PCR was performed in a 20- μ L reaction mixture consisting of 50 μ M KCl, 10 μ M Tris, 2 μ M MgCl₂, 0.2 μ M dNTP, 0.2 μ M of each primer, 1 unit of Taq DNA polymerase and 1 μ L of DNA matrix. The reaction conditions were as follows: initial denaturation at 95°C for 3 min; followed by 30 cycles of denaturation at 94°C for 30 s, annealing at 50°C for 30 s, and elongation at 72°C for 1 min; and a final elongation at 72°C for 7 min. Confirmation of amplification was carried out using agarose gel electrophoresis with ethidium bromide to detect the presence of DNA. Successful products were purified by ethanol precipitation and then were used as the template DNA for cycle sequencing reactions performed using a BigDye Terminator Cycle Sequencing Kit ver. 3.1 (Applied Biosystems) following the manufacturer's protocol; sequencing was conducted with ABI PRISM 3110 and 3500 (Applied Biosystems) automatic sequencers. Both DNA strands were sequenced to ensure accuracy. PCR and sequencing reactions for *Phoronis embryolabi* were conducted independently (on different days and purified and sequenced with different reaction plates) to avoid cross-contamination of the samples and reaction mixtures.

Sequence analysis

The *COI* sequences were edited, verified and aligned by eye using BioEdit software (Hall 1999). Several ingroup and outgroup (i.e. brachiopod) sequences were acquired from the National Centre of Biotechnology Information (NCBI) database. None of the obtained *COI* sequences contained insertions, deletions, or nonsense or stop codons, indicating that they did not result from PCR errors or sequencing errors and did not

represent pseudogenes or the *COI* of symbiotic organisms. The 28S sequences contained the indels, and we therefore used the Muscle algorithm as implemented in the MEGA6 software (Tamura *et al.* 2013) after the sequences were verified in BioEdit. The existence of any double peaks (i.e. peaks identical to or at least clustered with each other) in the chromatogram of the fragments was determined, and appropriate IUPAC codes were used. Sequence data were entered into NCBI, and the BLAST program was used to verify the species identity for each sequence. Orthologous positions containing obscure bases were excluded from the analyses using the pairwise deletion option. Sequence divergences (i.e. pairwise distances) among and within species were calculated using the *p*-distance method implemented in MEGA6 and the standard invertebrate mitochondrial genetic code. This distance was preferred because corrected models, for example, the Jukes–Cantor (JC) (Jukes and Cantor 1969) and Kimura-2-Parameter (K2P) distance (Kimura 1980), have been shown to be misleading in a DNA barcoding context (see Srivathsan and Meier 2012). Neighbour-joining (Saitou and Nei 1987) trees based on *p*-distances were created to provide a graphic representation of divergence patterns among and within species. Node support was assessed by the bootstrap method (Felsenstein 1985) using 1000 pseudoreplicates. Phylogenetic inference was performed for *COI*, 28S and concatenated *COI*+28S sequences using a Bayesian approach as implemented in MrBayes 3.2 software (Ronquist and Huelsenbeck 2003) with 10 million generations, the first 30% of which were discarded as burn-in; every 1000th generation was sampled. The nucleotide substitution model GTR+I+G was chosen for both fragments using the Bayesian information criterion, corrected Akaike information criterion and maximum likelihood (ML) metrics (Nei and Kumar 2000) in MEGA6. The trees were rooted with a

brachiopod outgroup, and we built unrooted trees to provide input data for subsequent PTP analysis.

Species delimitation

We used three methods for species delimitation and identification: comparison of tree topologies, automatic barcode gap discovery (ABGD) (Puillandre *et al.* 2012) and Poisson tree processes (PTP) (Zhang *et al.* 2013). The gene trees were separately calculated for both fragments using MEGA6 as explained above. The ABGD method is based on pairwise distances and detects breaks in the distribution, which are referred to as the 'barcode gaps' (Hebert *et al.* 2003), without any prior species hypothesis. The ABGD method is commonly used for species delimitation analyses (e.g. Jörger *et al.* 2012; Barco *et al.* 2013; Krug *et al.* 2013; Cámara *et al.* 2014), and the ABGD program is available at <http://www.wabi.snv.jussieu.fr/public/abgd/abgdweb.html> (accessed January 25, 2016). We analysed *COI* alignment using either the uncorrected *p*-distance or each of two available corrected JC and K2P distances; X-value was set to 0.2 and other settings were left as default. The PTP species delimitation test was run using the bPTP server <http://species.h-its.org/ptp/> with 500 000 generations and with other settings as default. An unrooted Bayesian phylogenetic tree inferred using concatenated *COI* and *28S* data (as described above) was used as the input tree. Two single NJ gene trees were used as input because polytomous Bayesian and ML trees did not fit the tree dichotomy requirement of the current algorithm implemented in the bPTP server.

Species-specific single nucleotide position (SNP) barcodes for *Phoronis embryolabi* were found using the character attribute organisation system (CAOS) approach (Sarkar *et al.* 2002, 2008; Bergmann *et al.* 2009) implemented in CAOS Workbench and available at <http://bol.uvm.edu/caos-workbench/caos.php> (accessed February 11, 2016). After diagnostic character states were extracted from molecular sequences using CAOS Analyzer software, CAOS Barcoder was used to create a CAOS barcode from the character attributes and group file.

Results

Phoronis embryolabi, sp. nov.

<http://zoobank.org/urn:lsid:zoobank.org:act:73C00AEE-E973-4283-B120-E6AC039F132E>

Actinotrocha sp. Temereva & Neretina, 2013: p. 622–633

Material examined

Two series of transverse sections, one series of longitudinal sections and two whole specimens were examined. Holotype: U. Ph. 2003, whole animal in the tube, fixed in 2.5% glutaraldehyde. Paratypes: U. Ph. 2004–2005, two series of transverse sections. Specimens (paratypes) used for sectioning had been previously photographed and fixed in 2.5% glutaraldehyde. Paratype: U. Ph. 2006, a portion of posterior body part, which was photographed and fixed in 96% ethanol for molecular study. All measurements (except the tube) are from paratypes U. Ph. 2004–2005. The holotype is kept at the Zoological Museum of the Moscow State University (Russia, Moscow). All paratypes are kept in the collection of Elena Temereva at the Department of Invertebrate Zoology of the biological faculty of Moscow State University (Russia, Moscow).

Description

Tube

The tube is 19 mm long (Fig. 1A). The body of the adult animal is red and can be observed through the tube wall. The anterior part of the tube is ~0.6 mm in diameter, and the posterior part is as much as 1.2 mm in diameter. The tube consists of an organic internal layer that is incrustated with sand grains (Fig. 1A). The tube is open at its anterior end and the opening is surrounded by debris of the inner organic layer (Fig. 1B). The posterior end of the tube lacks sand grains and consists of an organic layer that forms a closed sac (Fig. 1C).

Morphology

The live adult animal (paratype) has a body length of 9 mm (Fig. 1E). The body is subdivided into the lophophore, head region, median sphincter and posterior region (Figs 1E, 2A). The lophophore is horseshoe-shaped and bears 80–90 tentacles that are 1.2 mm long (Figs 1F, 3A). The lophophoral organs are located in the lophophoral concavity (Fig. 1F). These organs are large, glandular and sac-shaped, and contain a voluminous cavity (Fig. 3A, B). The head region is ~1 mm long (Fig. 1D). At the anterior end, the head region bears a prominent anal hill 58 µm high (Figs 1D, 3C). The head region is separated from the median sphincter by a deep, narrow furrow (Fig. 4A–C) that rests on a thick layer of cross muscles (Fig. 4C). The middle sphincter is 0.7 mm long and is characterised by a thick integument (Fig. 4A, D). The posterior region is the most extended part of the body and is 5 mm long (Fig. 1E) with a dense anterior portion characterised by a thick integument, and a posterior portion, which has a thin transparent integument (Fig. 1E). In *Phoronis embryolabi*, sp. nov., the ampulla, which is extremely prominent in many other phoronids (Temereva and Malakhov 2001), is completely indistinct.

The integument of the upper portion of the posterior region contains numerous glands with large dense granules (Figs 4E, 5A).

In the trunk coelom, there are five mesenteries: anal, oral, left and right lateral, and interintestinal. The anal and left lateral mesenteries extend between the body wall and the ascending branch of the digestive tract. The oral and right lateral mesenteries pass between the body wall and the descending branch of the digestive tract. The interintestinal mesentery connects the two branches of the digestive tract (Fig. 4D, E).

Organisation of the muscular system differs in different parts of the body. In the head region, the longitudinal muscle is organised as a few bundles (Figs 3E, 5B), each wide and short and consisting of 30–40 muscle cells (Fig. 5B). Two groups of small muscle cells (i.e. each with six or seven muscle cells) are located at the base of each bundle.

In the head region, the formula of longitudinal muscles is as follows (Fig. 3E):

4	6
4	6

In the median sphincter, the length of longitudinal muscle cells increases twice (Fig. 5C). The basal muscle cells, which are very

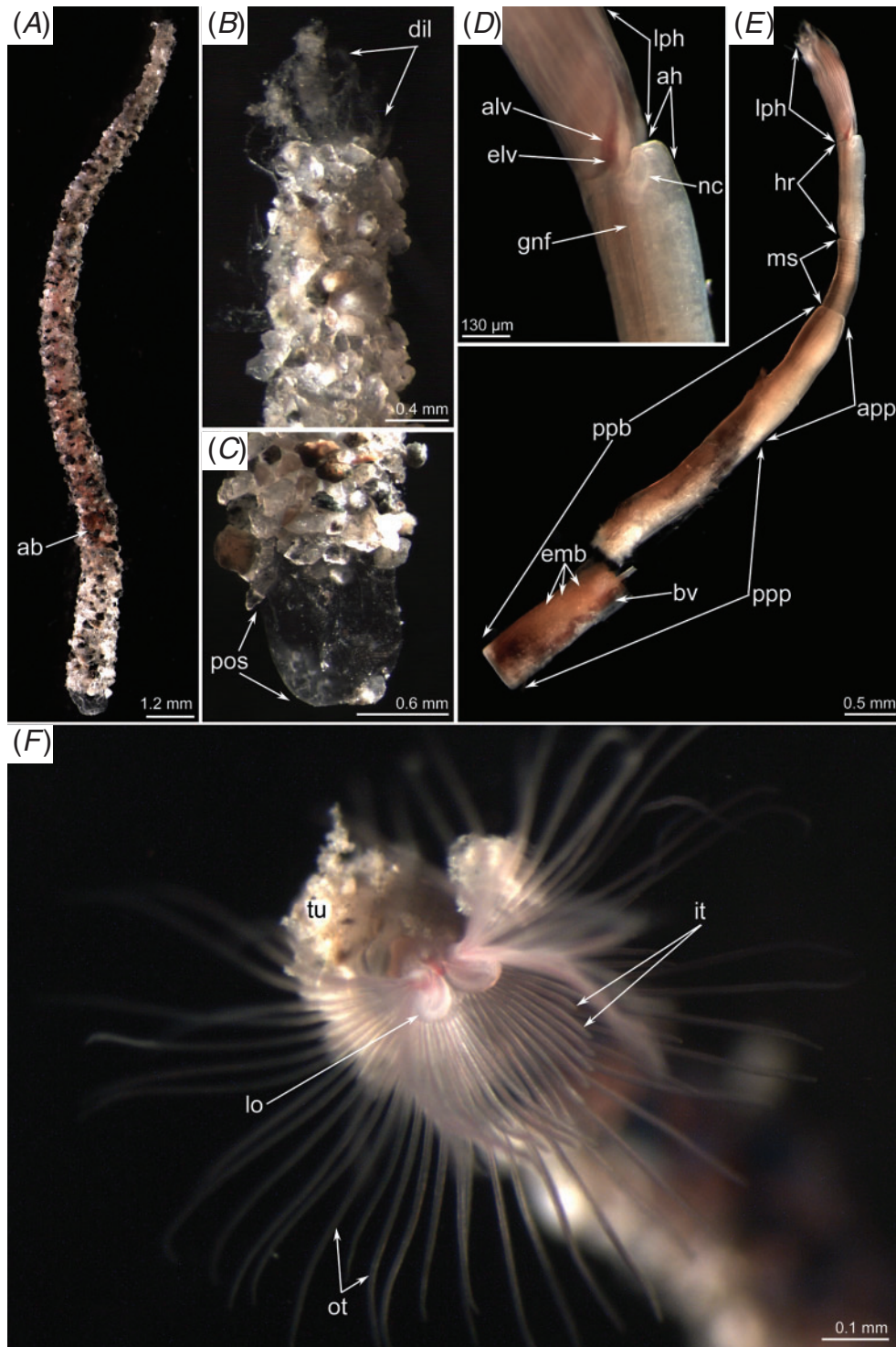


Fig. 1. *Phoronis embryolabi* (A–C) holotype U. Ph. 2003 and (D–F) paratype U. Ph. 2004. Photographs of (A–C, F) live and (D, E) fixed animals. (A) Overview of the tube with live animal inside; (B) the anterior portion of the tube; (C) the posterior portion of the tube; (D) the lophophore and the head region of the animal viewed from the left; (E) overview of animal from the left; (F) top view of the lophophore with paired lophophoral organs in the lophophoral concavity. Abbreviations: ab, animal body is visible through the tube; alv, afferent lophophoral blood vessel; ah, anal hill; app, anterior portion of the posterior region; bv, blood vessel; dil, debris of organic layer of tube; elv, efferent lophophoral vessel; emb, embryos; gnf, giant nerve fibre; hr, head region; it, inner tentacles; lo, lophophoral organ; lph, lophophore; ms, median sphincter; nc, nephridial canal; ot, outer tentacles; pos, posterior sac of tube organic layer; ppb, posterior region of the body; ppp, posterior portion of the posterior region; tu, tube.

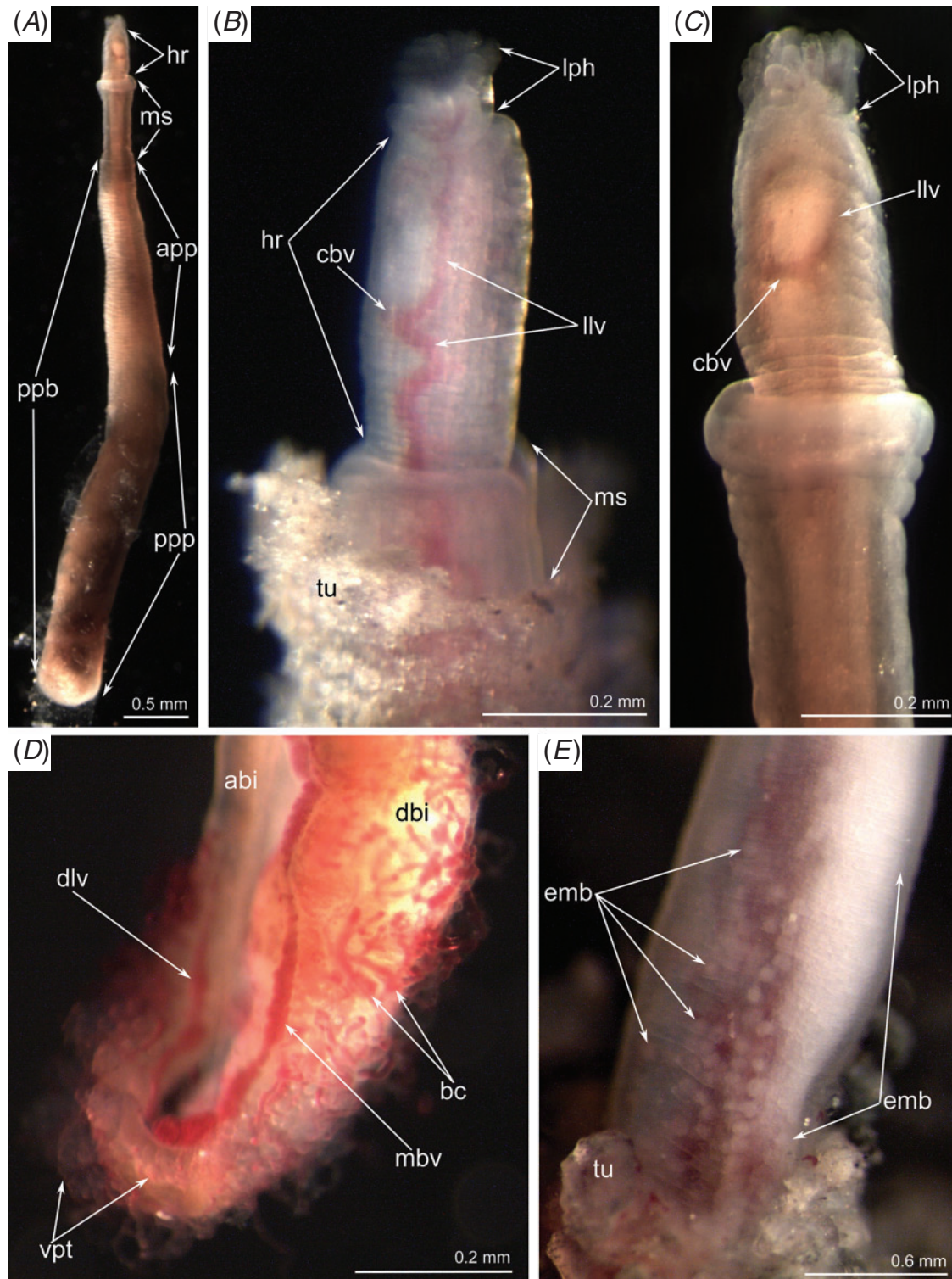


Fig. 2. *Phoronis embryolabi* (A–C) paratype U. Ph. 2005 and (D, E) paratype U. Ph. 2006. Photographs of (A, C) fixed and (B, D, E) live animals. (A) Whole animal viewed from the oral side; (B) head region and lophophore viewed from the left; (C) head region and lophophore viewed from the oral side; (D) posterior part of the digestive tract with the main blood vessels; (E) anterior portion of the posterior region: numerous embryos are visible through the integument. Abbreviations: abi, ascending branch of intestine; app, anterior portion of the posterior region; bc, blood caeca; cbv, ventral blood commissure; dbi, descending branch of intestine; dlv, dorso-lateral blood vessel; emb, embryos; hr, head region; llv, left lateral blood vessel; lph, lophophore; mbv, median blood vessel; ms, median sphincter; ppb, posterior region of the body; ppp, posterior portion of the posterior region; tu, tube; vpt, vasoperitoneal tissue.

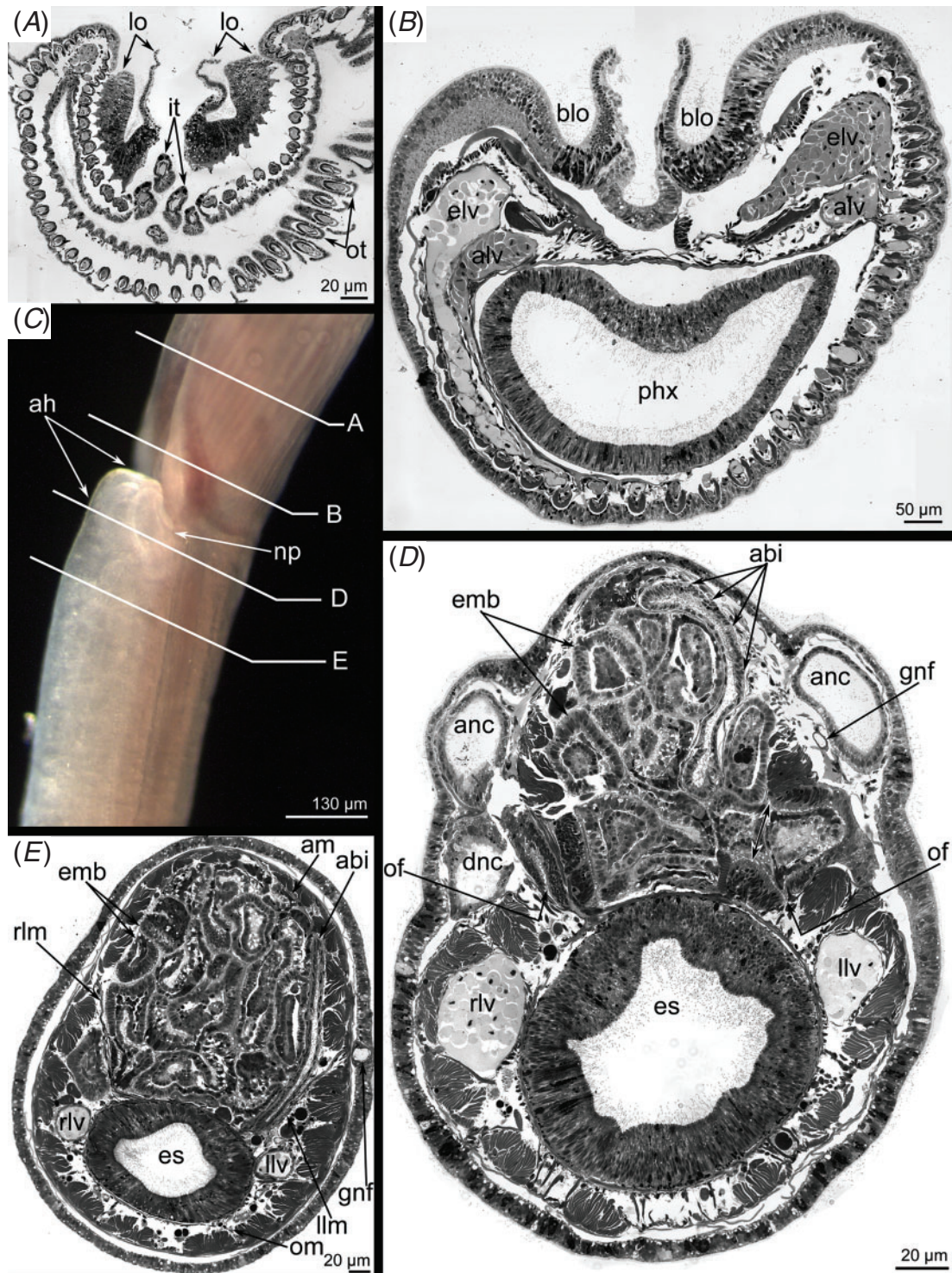


Fig. 3. *Phoronis embryolabi* paratype U. Ph. 2004. Photographs of (A, B, D–F) transverse semi-thin sections and (C) fixed animal. (A) Middle part of the lophophoral organs. (B) The base of the lophophoral organs and pharynx. (C) The lophophore and portion of the head region viewed from the right. The white lines indicate the levels of the sections. (D) Section through the nephridial canals: the anal funnel is marked by a double-sided arrow. (E) Section below the metanephridia. Abbreviations: abi, ascending branch of intestine; ah, anal hill; alv, afferent lophophoral blood vessel; am, anal mesentery; anc, ascending branch of nephridial canal; blo, base of lophophoral organ; dbi, descending branch of intestine; dnc, descending branch of nephridial canal; elv, efferent lophophoral vessel; emb, embryos; es, oesophagus; gnf, giant nerve fibre; hr, head region; it, inner tentacles; llv, left lateral blood vessel; llm, left lateral mesentery; lo, lophophoral organ; np, nephridiopore; of, oral funnel; om, oral mesentery; ot, outer tentacles; phx, pharynx; rlm, right lateral mesentery; rlv, right lateral blood vessel.

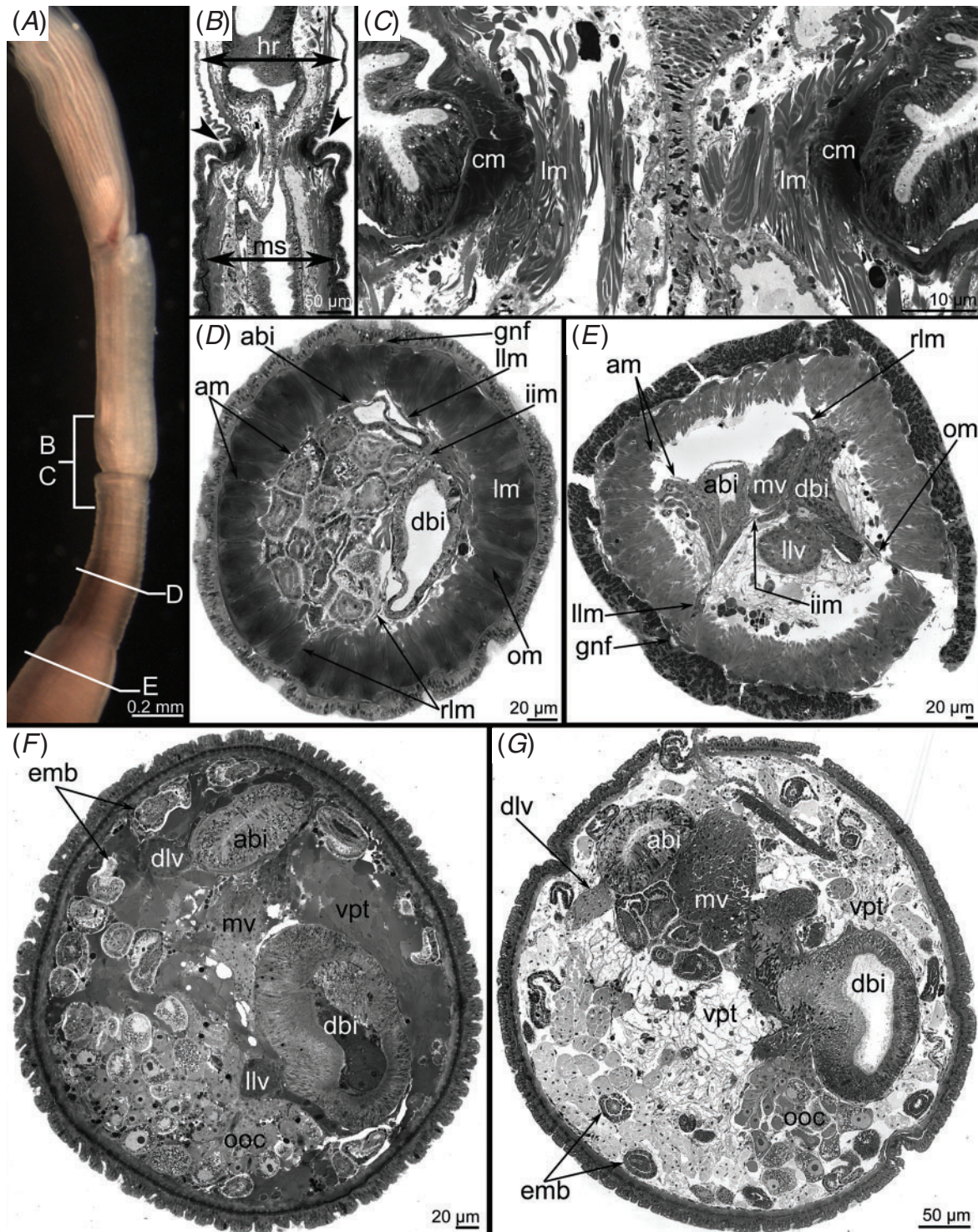


Fig. 4. *Phoronis embryolabi* (A–E, G) paratype U.Ph. 2004 and (F) paratype U.Ph. 2005. Photographs of (A) fixed animal and (B, C) longitudinal and (D–G) transverse semi-thin sections. (A) Anterior part of the body viewed from the right. White lines indicate the levels of the sections. (B) Section through the deep, narrow furrow between the head region and the median sphincter. (C) Organisation of musculature of the deep, narrow furrow between the head region and the median sphincter. (D) Median sphincter. (E) Anterior portion of the posterior region of the body. (F, G) Posterior portion of the posterior region of the body in (F) paratype U.Ph.2005 and (G) in paratype U.Ph.2004. Abbreviations: abi, ascending branch of intestine; am, anal mesentery; cm, circular muscles; dbi, descending branch of intestine; dlv, dorso-lateral blood vessel; emb, embryos; es, oesophagus; gnf, giant nerve fibre; hr, head region; iim, interintestinal mesentery; llv, left lateral blood vessel; llm, left lateral mesentery; lm, longitudinal muscles; ms, median sphincter; mv, median blood vessel; om, oral mesentery; ooc, oocytes; rlm, right lateral mesentery; vpt, vasoperitoneal tissue.

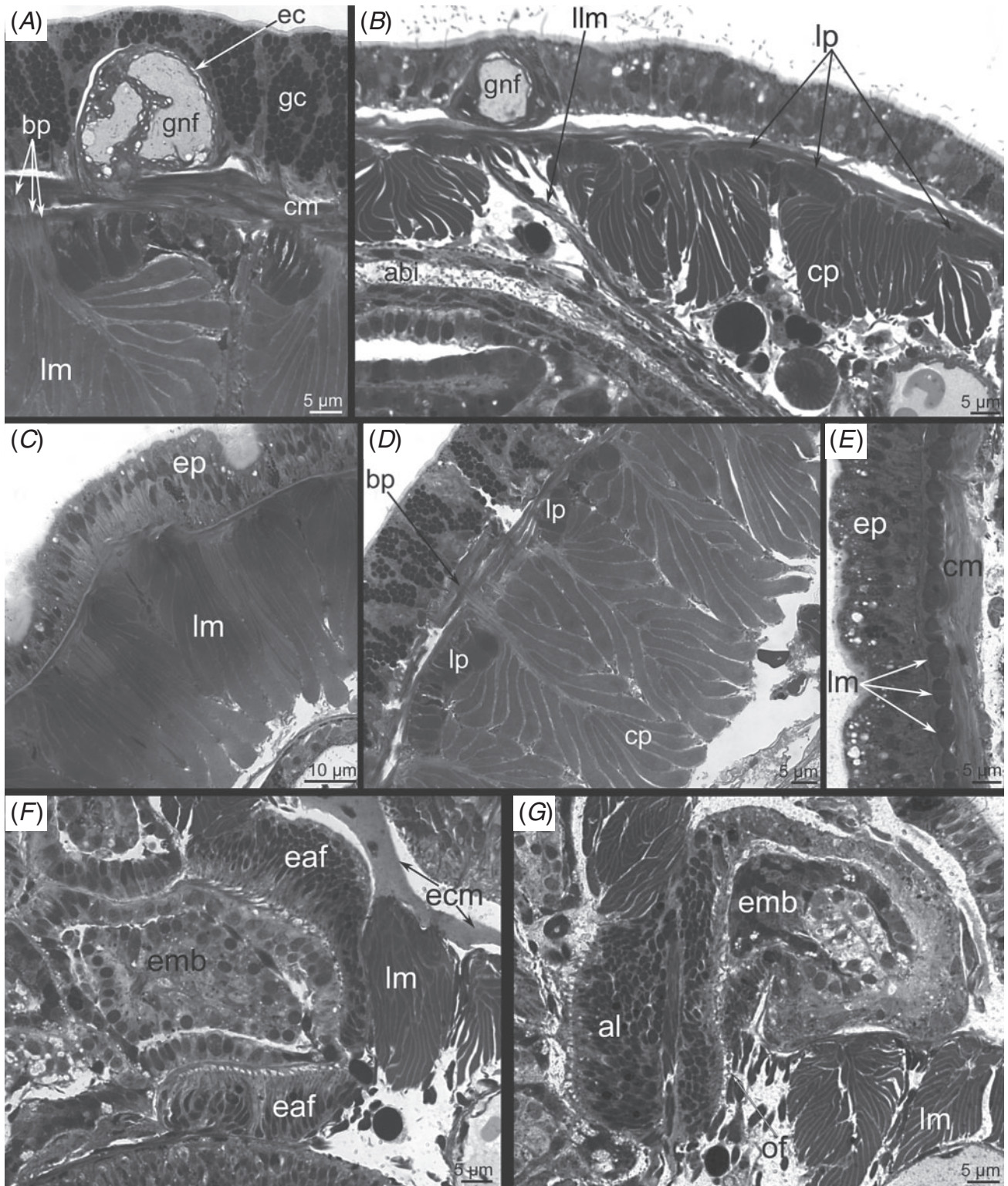


Fig. 5. *Phoronis embryolabi* paratype U. Ph. 2004. Photographs of transverse semi-thin sections. (A) Epithelium and giant nerve fibre in the anterior portion of the posterior region of the body; (B) muscles in the head region; (C) muscles of the median sphincter; (D) muscles of the anterior portion of the posterior region; (E) muscles of the posterior portion of the posterior region; (F) anal funnel of the left metanephridium with the embryo inside; (G) oral funnel of left metanephridium. Abbreviations: abi, ascending branch of intestine; al, anal lobe of anal funnel of metanephridium; bp, basal projections of longitudinal muscles; cm, circular muscles; cp, central part of muscle bundle; eaf, epithelium of anal funnel of metanephridium; ec, envelope cells; emb, embryos; ep, epithelium; gc, glandular cells; gnf, giant nerve fibre; llm, left lateral mesentery; lm, longitudinal muscles; lp, lateral part of bundle of longitudinal muscle.

short in the head region, become long. Thus, the longitudinal muscles form a continuous layer, and the bundles cannot be strictly distinguished. The approximate muscle formula is as follows (Fig. 4D):

$$\begin{array}{c|c} 10 & 10 \\ \hline 8 & 8 \end{array}$$

In the upper portion of the posterior region, longitudinal muscles form large feather-like bundles (Figs 4E, 5D). They have a central part and lateral parts, which are formed by short muscle cells (as in the head region). Muscle cells of the central part form basal projections, which pass within cells of the circular musculature and are anchored to the extracellular matrix (Fig. 5A, D). The muscle formula does not change (Fig. 4E).

In the lower portion of the posterior region, the muscle layers invert (i.e. the cross muscles are located above the longitudinal muscles) (Figs 4F, G, 5E). The longitudinal muscles consist of small cells, which are usually in groups of two or three.

The excretory system is represented by two metanephridia located in the head region (Figs 3D, 6A, B). Each metanephridium consists of a ciliated funnel and a curved excretory duct (Fig. 6C). The funnel has two openings: a large anal and a small oral (Figs 3D, 5F, G). The anal opening is supplied by a long, ciliated lobe, which extends along the lateral mesentery (Figs 5F, 6C). The duct consists of ascending and descending branches. At the level of the anus, the ascending branch bends and forms a large chamber, which opens by extended nephridiopore (Figs 3D, 6A, B). The nephridiopore is ~36 µm in diameter.

The blood system includes four longitudinal blood vessels: median, dorsolateral and two lateral. The left and right lateral blood vessels extend along the head region (Fig. 2D). On the border between the head region and the median sphincter, the left and right blood vessels merge (Fig. 2C). The dorsolateral vessel is well developed and can be observed in live animals and in cross-sections of the posterior region (Fig. 2C, 4F, G). The branched blood capillaries originate from the left lateral and dorsolateral vessels.

The nervous system includes a giant nerve fibre (Fig. 5A, B) in the left upper portion of the posterior region with a diameter $\sim 23 \pm 2$ µm (two individuals). Numerous cells form an envelope around the giant nerve fibre (Fig. 5A).

Phoronis embryolabi, sp. nov. is hermaphroditic. The vasoperitoneal tissue is developed in the lower portion of the posterior region, where it occupies the entire volume of the coelom (Fig. 4F, G). In paratype U. Ph.2004, cells of the vasoperitoneal tissue have light cytoplasm (Fig. 4G), whereas cells of paratype U. Ph.2005 have dense cytoplasm (Fig. 4F). Oocytes are located along the left lateral blood vessel in the lower portion of the posterior region (Fig. 4F, G). The mature oocyte is ~40 µm long (from the basal to the apical end). Although sperm are numerous in the trunk coelom and can even be found in the digestive tract of young embryos, which develop in the mother trunk, different stages of spermatogenesis and testis could not be found in the specimens with oocytes. However, this species has large lophophoral organs, which occur in hermaphroditic species or in males of dioecious species.

Development

Development is unusual in *Phoronis embryolabi*, sp. nov. in that it involves viviparity, with embryos developing in the trunk coelom (Fig. 4F, G).

The least mature embryos observed in this study were at the early gastrula stage (Fig. 7A). The early gastrula is ~26 µm long. The mesodermal cells immigrate from the walls of the archenteron, a closed cavity in the future pre-oral lobe, at the middle gastrula stage (Fig. 7B). The late gastrula has a prominent archenteron and muscle cells along the ventral side (Fig. 7C). In the early larva, the intestine is still closed, and the protonephridia develop as a single ventral invagination of the ectoderm (Fig. 7D). In the young completely formed larva, the intestine is complete, and the post-oral ciliated band begins to develop as a concentration of columnar cells (Fig. 7E). Larvae with a complete gut are 66 µm long and are ready to be released into the environment. They float into the anal chambers of the head region of the mother trunk coelom (Fig. 3D, E), where larvae are so numerous they are squashed together and their body shape is deformed.

Distribution and habitat

Phoronis embryolabi, sp. nov. lives commensally within the burrow of the thalassinidean shrimp *Nihonotrypaea japonica* (Ortmann, 1891). Burrow holes are located at a depth of 60 cm, and each burrow is ~2 m in length and made of sandy mud. In Vostok Bay, *P. embryolabi* was found in backwater Tihaya Zavod (42°54'0.36"N, 132°43'28.83"E).

Differential diagnosis

Phoronis embryolabi, sp. nov. is most similar to *Phoronis pallida* Silén, 1952, including several important features. First, the body of both species is divided into clear regions (Silén 1952). Second, both species have a horseshoe-shaped lophophore. Third, both species have an unusual type of longitudinal muscle (described by Silén (1952) as 'pallid musculature') and a similar muscle formula. Moreover, the muscle formula, which is one of the most important distinguishing features of phoronids (Selys-Longchamps 1907), is similar in different parts of the body of both species. The absence of variation in the number of longitudinal muscles is regarded as an important characteristic of *P. pallida* (Emig 1979). Silén reported that the muscle formula in the anterior region of *P. pallida*, which corresponds to the head region of *Phoronis embryolabi*, is:

$$\begin{array}{c|c} 5-6 & 5 \\ \hline 4 & 3-4 \end{array}$$

and in the 'second zone', which corresponds to the median sphincter of *Phoronis embryolabi*, is:

$$\begin{array}{c|c} 10 & 10 \\ \hline 8 & 8 \end{array}$$

Phoronis embryolabi has a similar arrangement of longitudinal muscles in the head region and the median sphincter, and in this regard is strikingly similar to *P. pallida*.

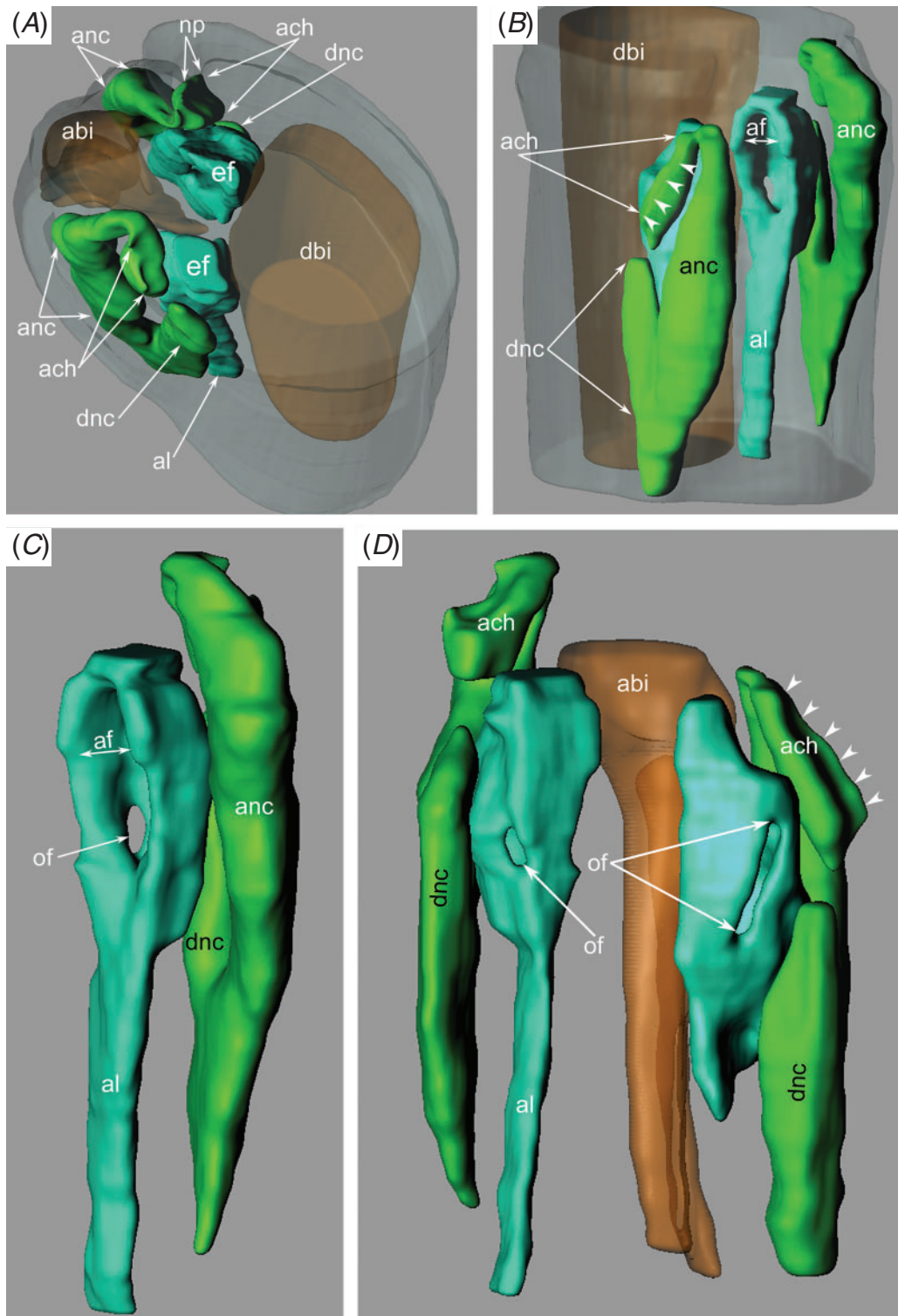


Fig. 6. *Phoronis embryolabi* paratype U. Ph. 2004: 3D-reconstructions of metanephridia and adjacent organs. The nephridiopore is marked by arrowheads. (A) Collocation of two nephridia, ascending and descending branches of intestine. Top-lateral view; (B) nephridia viewed from the left-anal side, the ascending branch of the intestine has been removed; (C) overview of the right metanephridium; (D) left and right metanephridia viewed from the oral side, the descending branch of intestine has been removed. Abbreviations: abi, ascending branch of intestine; ach, the chamber of ascending branch of nephridial canal; af, anal funnel; al, anal lobe; anc, ascending branch of nephridial canal; dbi, descending branch of intestine; dnc, descending branch of nephridial canal; ef, epithelium of funnel; np, nephridiopore; of, oral funnel.

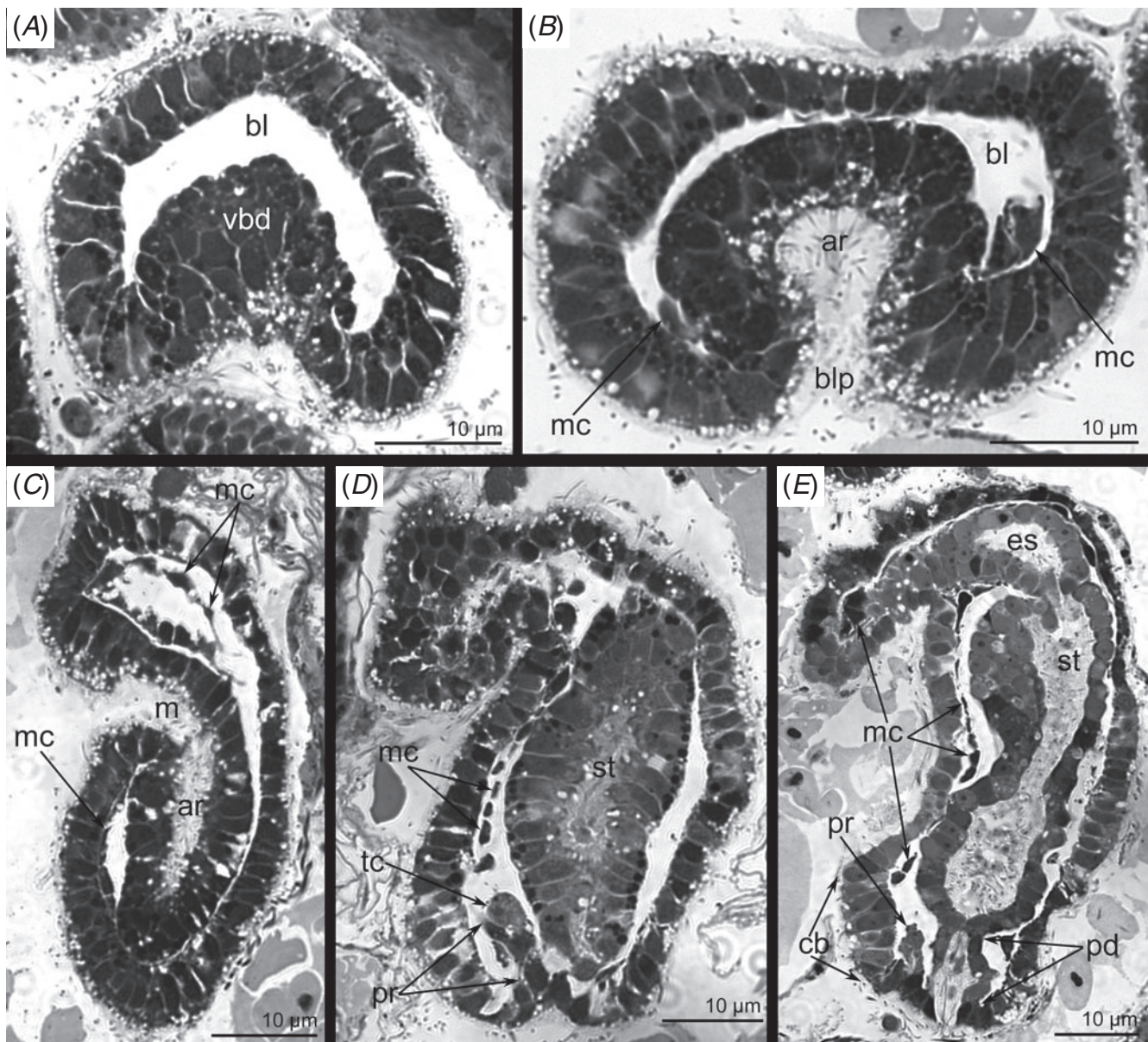


Fig. 7. *Phoronis embryolabi* paratype U. Ph. 2004: stages of development that occur in the mother's trunk coelom. Longitudinal semi-thin sections: (A) early gastrula; (B) middle gastrula; (C) late gastrula with prominent archenteron; (D) early larva with developed protonephridia; (E) young completely formed larva with through digestive tract, ciliated bands and protonephridia. Abbreviations: ar, archenteron; bl, blastocoel; blp, blastopore; cb, ciliated band; es, oesophagus; m, mouth; mc, mesodermal cell; pr, protonephridium; pd, proctodaeum; st, stomach; tc, terminal cell; vbd, blastoderm of vegetal pole.

However, there are many morphological differences between *P. pallida* and *P. embryolabi*. The body length is only ~10 mm for *P. embryolabi*, but is typically ~25 mm for *P. pallida* (Silén 1952) and can be as high as 140 mm for *P. pallida* (Bailey-Brock and Emig 2000). Although the bodies of both *P. pallida* and *P. embryolabi* exhibit prominent regionalisation, *P. pallida* has three sphincters and six parts of the body, whereas *P. embryolabi* has three parts of the body.

The organisation of the metanephridia also differs between the species. In *P. pallida*, nephridia have two pseudo-funnels (the anal is slightly larger than the oral funnel) and a nephridioduct, which is subdivided into descending and ascending branches. The

nephridiopore opens on an anal papilla at anus level (Emig 2016). In contrast, each metanephridium in *P. embryolabi* has a large anal funnel with a long anal lobe and a narrow oral funnel. The nephridioduct consists of descending and ascending branches. The ascending branch is curved and has a voluminous descending chamber, which opens on the lateral side of the body by lengthy nephridiopore, whose opening is ellipse-shaped. Such organisation of the nephridioduct correlates with viviparity in that the large, fully developed larvae are released into the environment through the large nephridiopore.

Phoronis pallida and *P. embryolabi* differ most in development. *Phoronis pallida* has classical holopelagic

development and releases fertilised eggs (Silén 1954; Emig 1977; Santagata 2002, 2004), whereas *P. embryolabi* is viviparous and releases completely formed actinotrochs into the environment. Viviparity has not been previously reported for phoronids. *Phoronis embryolabi* produces a huge number of small eggs. As suggested before (Temereva and Malakhov 2016), the combination of viviparity and a large number of eggs results in a large number of competent larvae that can complete metamorphosis in the burrows of shrimp.

Viviparity leads to the formation of very specific larvae in *P. embryolabi*. Among planktotrophic phoronid larvae, larvae of *P. embryolabi* have the smallest body size and the fewest tentacles. Larvae of *Phoronis pallida*, which according to morphological and molecular analysis is the closest relative, morphologically resemble *P. embryolabi* larvae (Santagata 2002). Detailed description of the morphology of *P. embryolabi* larvae from Vostok Bay is provided in a previous paper (Temereva and Neretina 2013).

Molecular diagnosis

Phoronis embryolabi clearly differs from known phoronid species in that it has six SNPs in the 28S marker (157T, 403C, 622T, 651T, 848C and 878G) and potentially 44 SNPs in the COI marker (Table 2). However, the COI sequences of its potentially closest relatives, *P. pallida* and *P. architecta*, were not analysed; hence, the number of barcoding SNPs in the COI marker may be less than 44.

Sequence data

A 615–618-bp fragment of COI and a 1005–1014-bp fragment of 28S were used for species delimitation and phylogenetic reconstruction in the Phoronida. Although a transition/transversion ratio (t_r/t_v ratio) of 0.97 in the COI fragment indicated no saturation bias in the most variable third position, the t_r/t_v ratio was rather high at the first position (Table 2). The mean nucleotide frequencies in the COI fragment were 17.8% (C), 36.1% (T/U), 24.7% (A) and 21.4% (G); in the 28S they were 20.3% (A), 17.5% (T/U), 28.4% (C) and 33.8% (G). These values are similar to those previously observed in this phylum. The whole dataset for both regions contained 1640 nucleotide positions with 693 variable sites, of which 383 were parsimony informative.

Species delimitation

In both gene trees (Fig. 8A, B), *P. embryolabi* constitutes a separate, well-supported cluster. No polymorphisms were detected in *P. embryolabi* COI and 28S sequences. Based on COI, *p*-distances (Table 3) between phoronid species ranged from 0.103 between *Phoronis australis* Haswell, 1883 1 and 2 to 0.277 between *P. embryolabi* and *Phoronis muelleri* Selys-Longchamps, 1903. Based on 28S (Table 4), interspecific *p*-distances ranged from 0.020 between *Phoronis viridis* Hilton, 1930 and *Phoronis ijimai* Oka, 1897 to 0.125 between *Phoronis emigi* Hirose, Fukiage, Katoh & Kajihara, 2014 and *Phoronis ovalis* Wright, 1856. The interspecific divergence

Table 2. Substitutions and nucleotide composition of Phoronida COI sequences

Abbreviations: tr, number of transitions; tv, transversions; tr/tv, transitions vs transversions ratio; f(N), nucleotide frequency

	Total positions	Invariable positions	tr	tv	tr/tv	f(T)	f(C)	f(A)	f(G)
Average	610.48	486	66	58	1.14	36.1	17.8	24.7	21.4
1st position	204	179	18	7	2.45	–	–	–	–
2nd position	203	197	2	3	0.67	–	–	–	–
3rd position	203.48	110	46	48	0.97	–	–	–	–

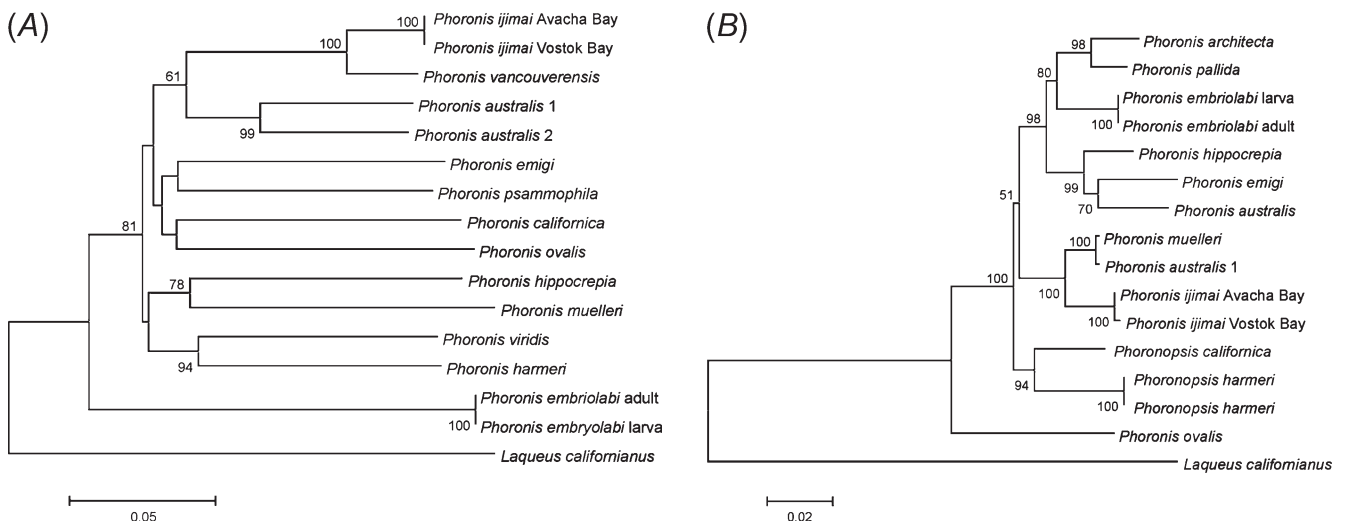


Fig. 8. Species delimitation: neighbour-joining, *p*-distance trees, bootstrap values >50% are shown at the internodes: (A) COI sequences; (B) 28S sequences.

Table 3. Uncorrected distances between *Phoronida COI* sequences (below diagonal) and standard errors (above diagonal)
Intraspecific divergences are underlined

	1	2	3	4	5	6	7	8	9	10	11	12	13	14	15
1 <i>Phoronis embryolabi</i> larva		0.000	0.018	0.018	0.017	0.018	0.018	0.018	0.018	0.017	0.017	0.017	0.017	0.017	0.018
2 <i>Phoronis embryolabi</i> adult	<u>0.000</u>		0.018	0.018	0.017	0.018	0.018	0.018	0.018	0.017	0.017	0.017	0.017	0.017	0.018
3 <i>Phoronis emigi</i>	0.249	0.249		0.016	0.016	0.016	0.017	0.016	0.015	0.016	0.016	0.016	0.016	0.017	0.017
4 <i>Phoronis australis</i> 1	0.252	0.252	0.185		0.012	0.016	0.017	0.016	0.015	0.015	0.014	0.015	0.016	0.016	0.016
5 <i>Phoronis australis</i> 2	0.246	0.246	0.183	0.103		0.017	0.017	0.016	0.015	0.015	0.015	0.015	0.016	0.016	0.016
6 <i>Phoronis hippocreptia</i>	0.257	0.257	0.201	0.208	0.214		0.016	0.017	0.017	0.016	0.016	0.016	0.017	0.016	0.017
7 <i>Phoronis muelleri</i>	0.277	0.277	0.227	0.226	0.234	0.198		0.017	0.016	0.017	0.017	0.017	0.017	0.017	0.017
8 <i>Phoronopsis californica</i>	0.267	0.267	0.201	0.190	0.185	0.218	0.229		0.016	0.016	0.016	0.016	0.016	0.016	0.016
9 <i>Phoronopsis psammophila</i>	0.256	0.256	0.178	0.178	0.164	0.213	0.206	0.203		0.016	0.016	0.016	0.016	0.016	0.016
10 <i>Phoronis ijimai</i> Vostok Bay	0.241	0.241	0.193	0.152	0.165	0.185	0.223	0.206	0.201		0.009	0.000	0.016	0.016	0.016
11 <i>Phoronis vancouverensis</i>	0.245	0.245	0.190	0.144	0.169	0.197	0.212	0.200	0.209	<u>0.051</u>		0.009	0.017	0.015	0.016
12 <i>Phoronis ijimai</i> Avacha Bay	0.241	0.241	0.193	0.152	0.165	0.185	0.223	0.206	0.201	<u>0.000</u>	<u>0.051</u>		0.016	0.016	0.016
13 <i>Phoronis ovalis</i>	0.246	0.246	0.201	0.195	0.191	0.231	0.239	0.200	0.193	0.198	0.210	0.198		0.017	0.017
14 <i>Phoronopsis viridis</i>	0.244	0.244	0.218	0.195	0.195	0.208	0.219	0.203	0.209	0.188	0.176	0.188	0.221		0.015
15 <i>Phoronopsis harmeri</i>	0.257	0.257	0.213	0.208	0.188	0.213	0.211	0.205	0.201	0.195	0.184	0.195	0.219	0.165	

Table 4. Uncorrected distances between *Phoronida 28S* sequences (below diagonal) and standard errors (above diagonal)
Intraspecific divergences are underlined

	1	2	3	4	5	6	7	8	9	10	11	12	13	14	15
1 <i>Phoronis embryolabi</i> larva		0.000	0.006	0.007	0.008	0.007	0.007	0.008	0.007	0.007	0.007	0.007	0.010	0.010	0.008
2 <i>Phoronis embryolabi</i> adult	<u>0.000</u>		0.006	0.007	0.008	0.007	0.007	0.008	0.007	0.007	0.007	0.007	0.010	0.010	0.008
3 <i>Phoronis pallida</i>	0.035	0.035		0.005	0.008	0.007	0.007	0.008	0.007	0.007	0.008	0.008	0.010	0.008	0.008
4 <i>Phoronis architecta</i>	0.048	0.048	0.025		0.007	0.007	0.008	0.008	0.008	0.008	0.008	0.008	0.010	0.011	0.009
5 <i>Phoronis emigi</i>	0.066	0.066	0.069	0.058		0.006	0.009	0.007	0.008	0.008	0.009	0.009	0.010	0.013	0.009
6 <i>Phoronis hippocreptia</i>	0.048	0.048	0.054	0.049	0.039		0.008	0.007	0.008	0.008	0.008	0.008	0.010	0.007	0.008
7 <i>Phoronopsis californica</i>	0.056	0.056	0.055	0.065	0.081	0.068		0.008	0.007	0.007	0.008	0.008	0.009	0.012	0.007
8 <i>Phoronis australis</i> 1	0.063	0.063	0.065	0.065	0.046	0.046	0.078		0.008	0.008	0.008	0.009	0.010	0.010	0.008
9 <i>Phoronis muelleri</i>	0.049	0.049	0.055	0.063	0.076	0.063	0.054	0.068		0.001	0.005	0.005	0.009	0.010	0.008
10 <i>Phoronis australis</i> 2	0.050	0.050	0.055	0.063	0.077	0.064	0.054	0.070	0.002		0.005	0.005	0.009	0.010	0.008
11 <i>Phoronis ijimai</i> Avacha Bay	0.054	0.054	0.061	0.065	0.084	0.063	0.062	0.078	0.025	0.026		0.001	0.009	0.009	0.008
12 <i>Phoronis ijimai</i> Vostok Bay	0.056	0.056	0.063	0.068	0.086	0.065	0.064	0.080	0.027	0.028	<u>0.002</u>		0.009	0.010	0.008
13 <i>Phoronis ovalis</i>	0.103	0.103	0.104	0.111	0.125	0.111	0.090	0.115	0.094	0.093	0.097	0.099		0.015	0.010
14 <i>Phoronopsis viridis</i>	0.028	0.028	0.016	0.032	0.043	0.012	0.035	0.028	0.024	0.024	0.020	0.028	0.063		0.000
15 <i>Phoronopsis harmeri</i>	0.066	0.066	0.065	0.074	0.080	0.064	0.049	0.078	0.064	0.064	0.065	0.067	0.101	<u>0.000</u>	

between the 28S sequences of *P. australis* 2 and *P. muelleri* was surprisingly low (Table 4; Fig. 8B) and was equal to the intraspecific distance between *P. ijimai* sequences. The interspecific divergence between the *COI* sequences of these species was greater than the average interspecific distance (0.203), which was 0.234 (Table 3; Fig. 8A).

ABGD analysis of the *COI* dataset run with the three available corrected and uncorrected distances along with PTP analysis of concatenated trees strictly delimited all available species including *Phoronis embryolabi* (Fig. 8). The PTP analysis of both single locus NJ trees supported *P. embryolabi* along with *P. ovalis*, *Phoronopsis harmeri* Pixell, 1912, *Phoronopsis californica* Hilton, 1930, and *P. ijimai* (Fig. 9).

CAOS analysis indicated that *P. embryolabi* has 6 and 44 single pure (*sPu*) character attributes in 28S and *COI* markers, respectively (Table 5). This indicates that *P. embryolabi* can be clearly barcoded using universal primers that can robustly amplify the short 28S marker containing *P. embryolabi*-specific single pure character attributes. We found that the short 28S sequences of the *Actinmotrocha* sp. in Temereva and Neretina (2013) (GenBank acc. # JX136703, JX136704, JX136705) were absolutely identical to our *P. embryolabi* sequences, and this included the same diagnostic positions #848 and #878 (Table 5) detected in our CAOS analysis. This

indicates that the unidentified species mentioned by Temereva and Neretina (2013) was *P. embryolabi*.

Etymology

'Embryolabi' stands for the **laboratory** of **embryology**. This name is devoted to the Laboratory of Embryology of the Institute of Marine Biology, Far East Branch, the Russian Academy of Sciences (Russia, Vladivostok). All members of the laboratory of embryology helped to organise the fieldwork at the Vostok Marine Biological Station. Much help was obtained from the head of the Laboratory of Embryology, Vladimir Yushin, and senior scientific researcher of Laboratory of Embryology Olga Yurchenko.

Phylogenetic analysis

Resulted 28S topologies possessed low bootstrap and posterior probability values because of high nucleotide divergence between the ingroup and outgroup including numerous gaps. These gaps led to considerable data loss due to exclusion of positions with gaps in MrBayes. Treatment of the gaps as a complementary binary dataset in Bayesian analyses did not significantly alter tree topology and posterior probabilities. Thus, single and concatenated trees resulted in different

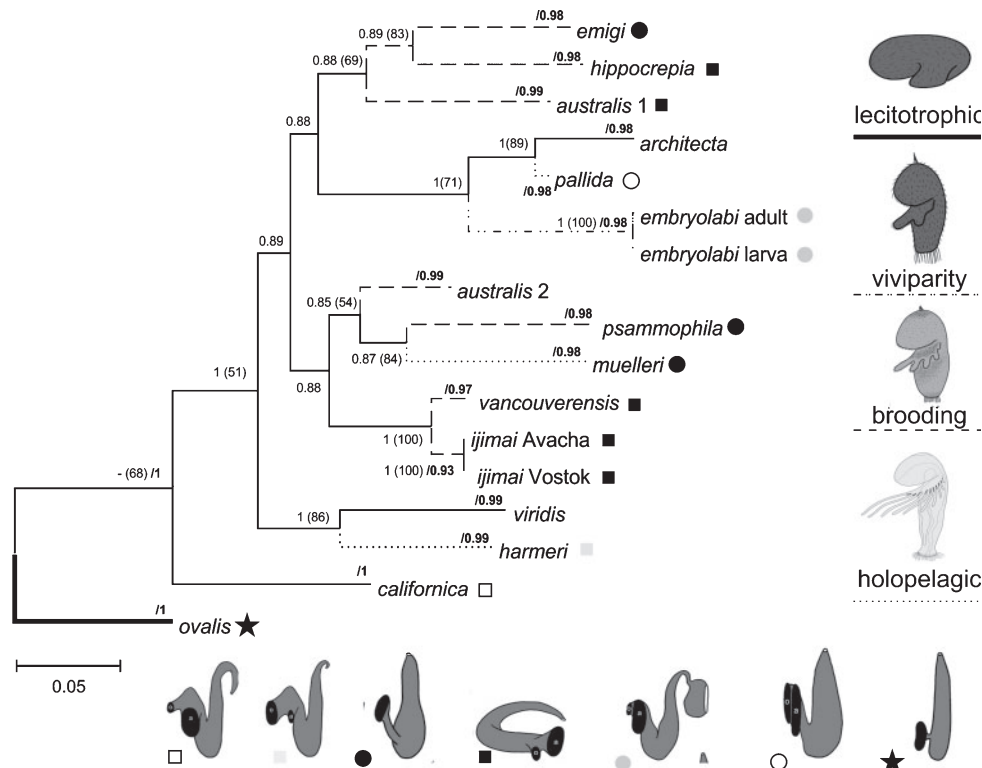


Fig. 9. Bayesian phylogenetic tree used in Poisson tree process (PTP) analysis, inferred from concatenated *COI* and 28S nucleotide sequence data (root *L. californianus* not shown, not used in PTP). Posterior probabilities are shown at the internodes; bootstrap indices above 50% (1000 replicates) obtained in maximum likelihood analysis are shown in parentheses; PTP acceptance indices >0.9 are marked in bold after the dash symbol at corresponding internal and terminal nodes. The types of development are indicated by branch colour, and metanephridial types are indicated by square colour.

topologies with dissimilar (although poorly supported) basal phoronid taxa. The sister clade of the other phoronids with the highest bootstrap support (68%) was found in the Bayesian concatenated tree for *P. ovalis* (Fig. 9). A similar topology was found in the 28S maximum parsimony (MP), ML and Bayesian trees (not shown, but the same as the NJ tree in Fig. 8B), although the COI MP, ML and Bayesian trees have *P. embryolabi* as the sister clade (the same as the NJ tree in Fig. 8A). Thus, we suppose *P. ovalis* is likely a sister clade of Phoronida. This hypothesis is supported by its untypical lecithotrophic development and unique morphological features (Emig 2016).

The 28S and concatenated trees suggested close phylogenetic relationships between *Phoronis embryolabi*, *P. pallida* and *P. architecta*, although this finding is not reflected by COI data because our COI dataset lacked the sequences for *P. pallida* and *P. architecta*. In the Bayesian tree, these three species formed a well-supported clade (Fig. 9) within the *Phoronis* clade and thus belong to the genus *Phoronis*. A quite different topology was inferred using COI data: when COI data were used, NJ (Fig. 8A), MP, ML and Bayesian (not shown, but the same topology as NJ) topologies had *P. embryolabi* in a sister-group position relative to the other Phoronida. The explanation of significant difference between the COI sequences of *P. embryolabi* and the other phoronids cannot be based on substitution saturation bias because of low $t_{\text{c}}/t_{\text{v}}$ ratios (Table 2) or based on morphology.

Discussion

In the Sea of Japan and adjacent waters (Aniva Bay), seven valid phoronid species had been found before the current study: *Phoronis ovalis* Wright, 1856; *P. muelleri* Selys-Longchamps, 1903; *P. psammophila* Cori, 1889; *P. hippocrepi* Wright, 1856; *P. ijimai* Oka, 1897; *Phoronopsis harmeri* Pixell, 1912; and *Phoronopsis albomaculata* Gilchrist, 1907 (Mamkaev 1962; Emig and Golikov 1990; Temereva 2005). According to our new results, the phoronid fauna of the Sea of Japan includes eight phoronid species.

Phoronid taxonomy is still poorly developed. Determination of phoronid species requires the preparation of several series of histological sections of different parts of the body. However, morphological features of adult phoronids vary greatly within one species and within different species and often depend on the season, geographic range and life cycle (Emig 1982). The variation in distinctive features probably reflects true differences between species: two valid species may be hidden under one recent name of species. This idea is supported by recent investigations of adult phoronids from different areas (Temereva and Malakhov 1999; Temereva 2000; Hirose *et al.* 2014) and by recent investigations of the diversity and distribution of phoronid larvae (Temereva and Neretina 2013; Temereva *et al.* 2016a, 2016b).

Phoronid taxonomy may be further elucidated by considering as many criteria as possible. Descriptions of species should include not only morphological and ecological features, but also details of embryonic and larval development. According to the peculiarities of development, two large clades can be established within phoronids. The first clade

includes phoronids with lecithotrophic development. At this time, lecithotrophy is known only for *Phoronis ovalis*, which has eggs with a diameter of 125 μm and lecithotrophic creeping larva. The second clade consists of phoronids with planktotrophic larvae and includes all other phoronid species whose development is known (Fig. 9). This clade is subdivided into three groups. Phoronids that brood embryos in the lophophoral concavity form the first group of the second clade. The four phoronid species in this group (*Phoronis ijimai*, *P. hippocrepi*, *P. australis* and *P. psammophila*) usually have eggs that are 100 μm in diameter and small, opaque larvae. The second group of the second clade is formed by phoronids with holopelagic development, which is definitely established in three phoronid species: *Phoronis muelleri*, *P. pallida* and *Phoronopsis harmeri*. In these phoronids, egg diameter ranges from 60 to 90 μm , and larvae are large and transparent. The third group in the second clade only contains *Phoronis embryolabi*, which releases completely developed larvae into the environment. This species has the smallest eggs (30–40 μm in diameter) and the smallest larvae (350 μm long).

The viviparity in *P. embryolabi* has much in common with the development of some bryozoans. Most bryozoans brood embryos in specialised polyps called ovicella, in which a special structure called the embryophore develops between the mother's tissue and the embryo (Ostrovsky 2013). In *P. embryolabi*, the embryophore is absent; however, embryos develop in the mother's coelom where they double in size. The increase in size suggests that the embryos obtain nutrition from the mother. In fully developed larvae with a complete intestine, nutrition occurs via the digestive tract, whereas early embryos obtain nutrition via cellular engulfing (pinocytosis) of nourishing coelomic liquid.

The arrangement of phoronid species into clades and groups according to type of development is not supported by either molecular or morphological analysis (Santagata and Cohen 2009; Hirose *et al.* 2014). The combination of molecular and morphological data reveals that the most prominent and valuable feature for phoronid taxonomy is the organisation of the metanephridia (Fig. 9). Adult phoronids exhibit five main types of organisation of metanephridia (Emig 1974, 1979; Temereva and Malakhov 2004) based on differences in the organisation of the funnel (nephrostome), the shape of the nephridioduct and the location of the nephropore. The first type of metanephridium it is the simplest metanephridia in *P. ovalis*, in which each metanephridium consists of a straight ascending duct with a single small nephrostome and a terminal nephropore opening on the anal papilla at the anus level. The second type of metanephridia organization is known in *Phoronis muelleri*, *P. psammophila* and *P. emigi*, in which each metanephridium has a single funnel and both descending and ascending branches of the nephridioduct. The third type of metanephridium is characterised by the presence of two funnels (the anal is larger than the oral) and an ascending duct that is extremely curved. This type of metanephridium occurs in *Phoronis ijimai*, *P. hippocrepi*, *P. australis* and *P. svetlanae*. The fourth type of metanephridia organisation has been described only in *Phoronis pallida*. This species has short descending and straight ascending branches of the duct; two large funnels open to the anal and oral chambers of the trunk

coelom. The fifth type of metanephridia organisation is considered the most complicated (Emig, 1974, 1979) and occurs in species of *Phoronopsis*. These species have a long nephridial duct with prominent descending and straight branches. In *Phoronopsis californica*, the upper portion of the ascending branch of the nephridioduct bends. This bend suggests a sixth type of metanephridia organisation, which is consistent with the unique phylogenetic position of *P. californica* relative to other phoronid species (Figs 8B, 9).

Conclusion

The taxonomy of phoronids remains unclear, but may be substantially clarified by the combined use of morphological, embryological and molecular data (Fig. 9). The development and organisation of larvae should be used as distinguishing features. According to recent analyses, the organisation of the metanephridia should be regarded as the morphological feature that is most useful for distinguishing phoronid species. For this reason, descriptions of new phoronid species require detailed information on the organisation of the metanephridia. Because the organisation of nephridia funnels depends on season, the structure of the nephridioduct has the most taxonomic utility.

The great variability of phoronid morphological features may reflect real differences among species, some not yet described. Indeed, this inference is supported by the existence of many morphotypes of phoronid larvae of unclear species identity (Ikeda 1901; Selys-Longchamps 1907; Forneris 1959; Johnson 2001; Johnson and Zimmer 2002; Temereva 2009; Temereva and Neretina 2013; Temereva *et al.* 2016b).

We cannot explain the significant difference between the *COI* sequence of *Phoronis embryolabi* and those of other phoronids by substitution saturation bias because of a low t_r/t_v ratio (Table 3) or by morphology. This difference also cannot occur due to sample contamination because, although the DNA was extracted and processed at different times from both adult and larval individuals, it always provided identical *COI* sequences.

Competing interests

The authors declare that they have no competing interests. All authors conceived the study and read and approved the final version of the manuscript.

Acknowledgements

We are very grateful to Konstantin Doodka (Russia, Vladivostok), who collected the specimens. ENT thanks the administration and the staff of the A.V. Zhirmunsky Institute of Marine Biology (Russia, Vladivostok) for help in organising and conducting the field studies. ENT is also very grateful to Vladimir Yushin and Olga Yurchenko for supplying all reagents and equipment for the field study. ENT thanks Elizaveta Nekiforova, who assiduously helped in the washing of the sediment, and Leonid Rusin, who diligently extracted some specimens from the tubes. Special thanks to Olga Chichvarkhina who contributed her efforts in DNA procedures. This research was supported in part by several grants. The collection of material was supported by the Russian Scientific Fund (#14-04-00262). The investigation of morphology was supported by the Russian Foundation for Basic Research (#15-04-20045; # 15-29-02601). 3D reconstructions were done with support from the Russian Scientific Fund (#14-50-00029). Molecular studies were supported by the Russian Foundation for Basic

Research (#14-04-00238). The processing of the paper was supported by Grants of the President of Russia (# MD-5812.2015.4). The participation of AC was supported by Far East Program grant #15-I-6-014o, DNA sequencing was supported by Russian Foundation for Basic Research grant #15-29-02456.

References

- Allcock, A. L., Barratt, I., Eléaume, M., Linse, K., Norman, M. D., Smith, P. J., Steinke, D., Stevens, D. W., and Strugnell, J. M. (2011). Cryptic speciation and the circumpolarity debate: a case study on endemic Southern Ocean octopuses using the COI barcode of life. *Deep-Sea Research. Part II, Topical Studies in Oceanography* **58**, 242–249. doi:10.1016/j.dsr2.2010.05.016
- Bailey-Brock, J. H., and Emig, C. (2000). Hawaiian Phoronida (Lophophorata) and their distribution in the Pacific region. *Pacific Science* **54**, 119–126.
- Barco, A., Houart, R., Bonomolo, G., Crocetta, F., and Oliverio, M. (2013). Molecular data reveal cryptic lineages within the northeastern Atlantic and Mediterranean small mussel drills of the *Ocenebrina edwardsii* complex (Mollusca: Gastropoda: Muricidae). *Zoological Journal of the Linnean Society* **169**, 389–407. doi:10.1111/zoj.12069
- Barr, N. B., Cook, A., Elder, P., Molongoski, J., Prasher, D., and Robinson, D. G. (2009). Application of a DNA barcode using the 16S rRNA gene to diagnose pest *Arion* species in the USA. *The Journal of Molluscan Studies* **75**, 187–191. doi:10.1093/mollus/eyn047
- Becker, S., Hanner, R., and Steinke, D. (2011). Five years of FISH-BOL: brief status report. *Mitochondrial DNA* **22**(Suppl. 1), 3–9. doi:10.3109/19401736.2010.535528
- Bergmann, T., Hadrys, H., Breves, G., and Schierwater, B. (2009). Character-based DNA barcoding: a superior tool for species classification. *Berliner und Munchener Tierarztliche Wochenschrift* **122**, 446–450.
- Brower, A. V. Z. (2006). Problems with DNA barcodes for species delimitation: 'ten species' of *Astraptes fulgerator* reassessed (Lepidoptera: Hesperidae). *Systematics and Biodiversity* **4**, 127–132. doi:10.1017/S147720000500191X
- Cámara, S., Carmona, L., Cella, K., Ekimova, I., Martynov, A., and Cervera, J. L. (2014). *Tergipes tergipes* (Forsk., 1775) (Gastropoda: Nudibranchia) is an amphiatlantic species. *The Journal of Molluscan Studies* **80**(5), 642–646. doi:10.1093/mollus/eyu015
- Chen, J., Li, Q., Kong, L. F., and Yu, H. (2011). How DNA barcodes complement taxonomy and explore species diversity: the case study of a poorly understood marine fauna. *PLoS One* **6**(6), e21326. doi:10.1371/journal.pone.0021326
- Clare, E. L., Lim, B. K., Engstrom, M. D., Eger, J. L., and Hebert, P. D. N. (2007). DNA barcoding of Neotropical bats: species identification and discovery within Guyana. *Molecular Ecology Notes* **7**, 184–190. doi:10.1111/j.1471-8286.2006.01657.x
- Collins, R. A., and Cruickshank, R. H. (2012). The seven deadly sins of DNA barcoding. *Molecular Ecology Resources* **13**(6), 969–975.
- Collins, R. A., Armstrong, K. F., and Meier, R. (2012). Barcoding and border biosecurity: identifying cyprinid fishes in the aquarium trade. *PLoS One* **7**, e28381. doi:10.1371/journal.pone.0028381
- DeSalle, R. (2006). Species discovery versus species identification in DNA barcoding efforts: response to Rubinoff. *Conservation Biology* **20**, 1545–1547. doi:10.1111/j.1523-1739.2006.00543.x
- DeSalle, R., Egan, M. G., and Siddall, M. (2005). The unholy trinity: taxonomy, species delimitation and DNA barcoding. *Philosophical Transactions of the Royal Society of London. Series B, Biological Sciences* **360**, 1905–1916. doi:10.1098/rstb.2005.1722
- Ekimova, I., Korshunova, T., Schechetov, D., Neretina, T., Sanamyan, N., and Martynov, A. (2015). Integrative systematics of Northern and Arctic nudibranchs of the genus *Dendronotus* (Mollusca, Gastropoda) with descriptions of three new species. *Zoological Journal of the Linnean Society* **173**(4), 841–886. doi:10.1111/zoj.12214

- Emig, C. C. (1974). The systematics and evolution of the phylum Phoronida. *Zeitschrift für Zoologische Systematik und Evolutionsforschung* **12**, 128–151.
- Emig, C. (1977). Embryology of Phoronida. *American Zoologist* **17**, 21–37. doi:10.1093/icb/17.1.21
- Emig, C. (1979). British and other phoronides. *Synopsis of the British Fauna* **13**, 1–57.
- Emig, C. (1982). The biology of Phoronida. *Advances in Marine Biology* **19**, 1–89. doi:10.1016/S0065-2881(08)60086-3
- Emig, C. (2016). Phoronid@ 2016. 31.11.2016. Available at: <http://paleopolis.rediris.es/Phoronida/>
- Emig, C., and Golikov, A. (1990). On phoronids of the Far Eastern seas of the USSR and their distribution in the Pacific Ocean. Зоологический журнал **69**, 22–30. [In Russian with English summary]
- Felsenstein, J. (1985). Confidence limits on phylogenies: an approach using the bootstrap. *Evolution* **39**, 783–791. doi:10.2307/2408678
- Feng, Y. W., Li, Q., Kong, L. F., and Zheng, X. D. (2011). COI-based DNA barcoding of Arcoida species (Bivalvia: Pteriomorpha) along the coast of China. *Molecular Ecology Resources* **11**, 435–441. doi:10.1111/j.1755-0998.2010.02975.x
- Folmer, O., Black, M., Hoeh, W., Lutz, R., and Vrijenhoek, R. (1994). DNA primers for amplification of mitochondrial cytochrome c oxidase subunit I from diverse metazoan invertebrates. *Molecular Marine Biology and Biotechnology* **3**, 294–299.
- Formeris, L. (1959). Phoronidea from Brazil. *Boletim Instute de Oceanography* **10**(2), 1–105.
- Goldstein, P. Z., and DeSalle, R. (2011). Integrating DNA barcode data and taxonomic practice: determination, discovery and description. *BioEssays* **33**, 135–147. doi:10.1002/bies.201000036
- Gouyé de Bellocq, J., Ferte, H., Depaquit, J., Justine, J.-L., Tillier, A., and Durette-Desset, M.-C. (2001). Phylogeny of the Trichostrongylina (Nematoda) inferred from 28S rDNA sequences. *Molecular Phylogenetics and Evolution* **19**(3), 430–442. doi:10.1006/mpev.2001.0925
- Hall, T. A. (1999). BioEdit: a user-friendly biological sequence alignment editor and analysis program for Windows 95/98/NT. *Nucleic Acids Symposium Series* **41**, 95–98.
- Hebert, P. D. N., and Gregory, T. R. (2005). The promise of DNA barcoding for taxonomy. *Systematic Biology* **54**, 852–859. doi:10.1080/10635150500354886
- Hebert, P., Cywinska, A., Ball, S., and de Waard, J. (2003). Biological identifications through DNA barcodes. *Proceedings. Biological Sciences* **270**, 313–321. doi:10.1098/rspb.2002.2218
- Hebert, P. D. N., Penton, E. H., Burns, J. M., Janzen, D. H., and Hallwachs, W. (2004a). Ten species in one: DNA barcoding reveals cryptic species in the neotropical skipper butterfly *Astraptes fulgerator*. *Proceedings of the National Academy of Sciences of the United States of America* **101**, 14812–14817. doi:10.1073/pnas.0406166101
- Hebert, P. D. N., Stoeckle, M. Y., Zemlack, T. S., and Francis, C. M. (2004b). Identification of birds through DNA barcodes. *PLoS Biology* **2**, e312. doi:10.1371/journal.pbio.0020312
- Hirose, M., Fukiage, R., Katoh, T., and Kajihara, H. (2014). Description and molecular phylogeny of a new species of *Phoronis* (Phoronida) from Japan, with a redescription of topotypes of *P. ijimai* Oka, 1897. *ZooKeys* **398**, 1–31. doi:10.3897/zookeys.398.5176
- Ikeda, I. (1901). Observation on the development, structure and metamorphosis of Actinotrocha. *Journal of the College of Science. Imperial University, Tokyo* **13**, 507–591.
- Ikeda, I. (1903). On the development of the sexual organs and their products in *Phoronis*. *Annotationes Zoologicae Japonenses* **3**, 141–153.
- Johnson, K. B. (2001). Phoronida. In 'An Identification Guide to the Larval Marine Invertebrates of the Pacific Northwest'. (Ed. A. L. Shanks.) pp. 251–257. (Oregon State University Press: Corvallis, OR.)
- Johnson, K. B., and Zimmer, R. L. (2002). Phylum Phoronida. In 'Atlas of marine invertebrate larvae'. (Eds C. Young, M. Rice, M. Sewell.) pp. 429–439. (Academic Press: San Diego, San Francisco, CA.)
- Jörger, K. M., Norenburg, J. L., Wilson, N. G., and Schrödl, M. (2012). Barcoding against a paradox? Combined molecular species delineations reveal multiple cryptic lineages in elusive meiofaunal sea slugs. *BMC Evolutionary Biology* **12**, 245. doi:10.1186/1471-2148-12-245
- Jukes, T. H., and Cantor, C. R. (1969). Evolution of protein molecules. In 'Mammalian Protein Metabolism'. (Ed. H. N. Munro.) pp. 21–132. (Academic Press: New York, NY.)
- Kimura, M. (1980). A simple method for estimating evolutionary rate of base substitutions through comparative studies of nucleotide sequences. *Journal of Molecular Evolution* **16**, 111–120. doi:10.1007/BF01731581
- Krug, P. J., Vendetti, J. E., Rodriguez, A. K., Retana, J. N., Hirano, Y. M., and Trowbridge, C. D. (2013). Integrative species delimitation in photosynthetic sea slugs reveals twenty candidate species in three nominal taxa studied for drug discovery, plastid symbiosis or biological control. *Molecular Phylogenetics and Evolution* **69**, 1101–1119. doi:10.1016/j.ympev.2013.07.009
- Lowenstein, J. H., Burger, J., Jeitner, C. W., Amato, G., Kolokotronis, S. O., and Gochfeld, M. (2010). DNA barcodes reveal species-specific mercury levels in tuna sushi that pose a health risk to consumers. *Biology Letters* **6**, 692–695. doi:10.1098/rsbl.2010.0156
- Mamkaev, Y. V. (1962). About Phoronids of Far Eastern seas. *Researches of Far East Seas USSR* **8**, 219–237. [In Russian with English summary]
- Meier, R. (2008). DNA sequences in taxonomy: opportunities and challenges. In 'The New Taxonomy'. (Ed. Q. D. Wheeler.) pp. 95–127. (CRC Press: New York, NY.)
- Meier, R., Shiyang, K., Vaidya, G., and Ng, P. K. (2006). DNA barcoding and taxonomy in Diptera: a tale of high intraspecific variability and low identification success. *Systematic Biology* **55**(5), 715–728. doi:10.1080/10635150600969864
- Nei, M., and Kumar, S. (2000). 'Molecular Evolution and Phylogenetics.' (Oxford University Press: New York, NY.)
- Ostrovsky, A. N. (2013). 'Evolution of Sexual Reproduction in Marine Invertebrates. Example of Gymnolaemate Bryozoans.' (Springer: Dordrecht, Heidelberg, New York, London.)
- Pons, J., Barraclough, T. G., Gomez-Zurita, J., Cardoso, A., Duran, D. P., Hazell, S., Kamoun, S., Sumlin, W. D., and Vogler, A. P. (2006). Sequence-based species delimitation for the DNA taxonomy of undescribed insects. *Systematic Biology* **55**(4), 595–609. doi:10.1080/10635150600852011
- Puillandre, N., Lambert, A., Brouillet, S., and Achaz, G. (2012). ABGD, automatic barcode gap discovery for primary species delimitation. *Molecular Ecology* **21**, 1864–1877. doi:10.1111/j.1365-294X.2011.05239.x
- Rattenbury, J. C. (1953). Reproduction in *Phoronopsis viridis*. The annual cycle in the gonads, maturation and fertilization of the ovum. *The Biological Bulletin* **104**, 182–196. doi:10.2307/1538792
- Ronquist, F., and Huelsenbeck, J. P. (2003). MRBAYES 3: Bayesian phylogenetic inference under mixed models. *Bioinformatics* **19**, 1572–1574. doi:10.1093/bioinformatics/btg180
- Saitou, N., and Nei, M. (1987). The neighbor-joining method: a new method for reconstructing phylogenetic trees. *Molecular Biology and Evolution* **4**, 406–425.
- Santagata, S. (2002). Structure and metamorphic remodeling of the larval nervous system and musculature of *Phoronis pallida* (Phoronida). *Evolution & Development* **4**(1), 28–42. doi:10.1046/j.1525-142x.2002.01055.x
- Santagata, S. (2004). A waterborne behavioral cue for the actinotroch larvae of *Phoronis pallida* (Phoronida) produced by *Upogebia pugettensis* (Decapoda: Thalassinidea). *The Biological Bulletin* **207**, 103–115. doi:10.2307/1543585

- Santagata, S., and Cohen, B. (2009). Phoronid phylogenetics (Brachiopoda: Phoronata): evidence from morphological cladistics, small and large subunit rDNA sequences, and mitochondrial *cox1*. *Zoological Journal of the Linnean Society* **157**, 34–50. doi:10.1111/j.1096-3642.2009.00531.x
- Sarkar, I. N., Thornton, J. W., Planet, P. J., Figurski, D. H., Schierwater, B., and DeSalle, R. (2002). An automated phylogenetic key for classifying homeoboxes. *Molecular Phylogenetics and Evolution* **24**, 388–399. doi:10.1016/S1055-7903(02)00259-2
- Sarkar, I. N., Planet, P. J., and DeSalle, R. (2008). CAOS software for use in character-based DNA barcoding. *Molecular Ecology Resources* **8**, 1256–1259. doi:10.1111/j.1755-0998.2008.02235.x
- Schindel, D. E., and Miller, S. E. (2005). DNA barcoding a useful tool for taxonomists. *Nature* **435**, 17. doi:10.1038/435017b
- Selys-Longchamps, M. (1907). 'Fauna und Flora des Golfes von Neapel und der Meeres-abschnitte: *Phoronis*.' (von R. Friedländer & Sohn: Berlin.) Monogr. 30, 280 S.
- Silén, L. (1952). Researches on Phoronidea of the Gullmar Fiord area (west coast of Sweden). *Arkiv för Zoologi* **4**(4), 95–140.
- Silén, L. (1954). Developmental biology of Phoronidea of the Gullmar Fiord area (west coast of Sweden). *Acta Zoologica* **35**, 215–257. doi:10.1111/j.1463-6395.1954.tb00035.x
- Sin, Y. W., Yau, C., and Chu, K. H. (2009). Morphological and genetic differentiation of two loliginid squids, *Uroteuthis (Photololigo) chinensis* and *Uroteuthis (Photololigo) edulis* (Cephalopoda: Loliginidae) in Asia. *Journal of Experimental Marine Biology and Ecology* **369**, 22–30. doi:10.1016/j.jembe.2008.10.029
- Sonnenberg, R., Nolte, A. W., and Tautz, D. (2007). An evaluation of LSU rDNA D1–D2 sequences for their use in species identification. *Frontiers in Zoology* **4**(1), 6–12. doi:10.1186/1742-9994-4-6
- Srivathsan, A., and Meier, R. (2012). On the inappropriate use of Kimura-2-parameter (K2P) divergences in the DNA-barcoding literature. *Cladistics* **28**(2), 190–194. doi:10.1111/j.1096-0031.2011.00370.x
- Tamura, K., Stecher, G., Peterson, D., Filipiński, A., and Kumar, S. (2013). MEGA6: molecular evolutionary genetics analysis version 6.0. *Molecular Biology and Evolution* **30**, 2725–2729. doi:10.1093/molbev/mst197
- Temereva, E. N. (2000). New Phoronid species *Phoronopsis malakhovi* (Lophophorata, Phoronida) from the South China Sea. *Зоологический журнал* **79**(9), 1088–1093.
- Temereva, E. N. (2005). Phylum Phoronids. In 'Biota of the Russian Basin of the Sea of Japan. Vol. 3. Brachiopoda and Phoronida'. (Ed. A. V. Adrianov.) pp. 50–136. (Dalnauka: Vladivostok.)
- Temereva, E. N. (2009). New data on distribution, morphology and taxonomy of phoronid larvae (Phoronida, Lophophorata). *Invertebrate Zoology* **6**(1), 47–64.
- Temereva, E. N., and Malakhov, V. V. (1999). A new rock dwelling phoronid species, *Phoronis svetlanae* (Lophophorata, Phoronida) from the Sea of Japan. *Зоологический журнал* **78**(5), 626–630.
- Temereva, E. N., and Malakhov, V. V. (2001). The morphology of the phoronid *Phoronopsis harmeri*. *Russian Journal of Marine Biology* **27**(1), 21–30. doi:10.1023/A:1018829722129
- Temereva, E. N., and Malakhov, V. V. (2004). Distinctive features of the microscopical anatomy and ultrastructure of the metanephridia *Phoronopsis harmeri*, Pixell, 1912 (Phoronida, Lophophorata). *Invertebrate Zoology* **1**(1), 93–103.
- Temereva, E. N., and Malakhov, V. V. (2006). Microscopic anatomy and ultrastructure of the lophophoral organs and adjacent epitheliums of the lophophoral concavity and anal papilla of *Phoronopsis harmeri* Pixell, 1912 (Lophophorata, Phoronida). *Russian Journal of Marine Biology* **32**(3), 134–141.
- Temereva, E. N., and Malakhov, V. V. (2007). Embryogenesis and larval development of phoronid *Phoronopsis harmeri* Pixell, 1912: dual origin of the coelomic mesoderm. *Invertebrate Reproduction and Development* **50**(2), 57–66.
- Temereva, E., and Malakhov, V. (2012). Embryogenesis in phoronids. *Invertebrate Zoology* **8**(1), 1–39.
- Temereva, E., and Malakhov, V. (2016). Viviparity of larvae is the new type of development in phoronids (Lophophorata: Phoronida). *Doklady Akademy of Science* **467**(3), 1–4.
- Temereva, E. N., and Neretina, T. V. (2013). A distinct phoronid larva: morphological and molecular evidence. *Invertebrate Systematics* **27**(6), 622–633.
- Temereva, E. N., Neretina, T. V., and Stupnikova, A. N. (2016a). An original description of the larval stages of *Phoronis australis* Haswell, 1883 and analysis of the world fauna of phoronid larvae. *Russian Journal of Marine Biology* **42**(2), 128–138. doi:10.1134/S1063074016020127
- Temereva, E. N., Neretina, T. V., and Stupnikova, A. N. (2016b). The fauna of the South China Sea include unknown phoronid species: new records of larvae and adults. *Systematics and Biodiversity* **14**(5). doi:10.1080/14772000.2016.1173739509523
- Turanov, S. V., and Kartavtsev, Y. P. (2014). The taxonomic composition and distribution of sand lances from the genus *Ammodytes* (Perciformes: Ammodytidae) in the North Pacific. *Journal of Marine Biology* **40**, 447–454.
- Undheim, E. A. B., Norman, J. A., Thoen, H. H., and Fry, B. G. (2010). Genetic identification of Southern Ocean octopod samples using mtCOI. *Comptes Rendus Biologies* **333**, 395–404. doi:10.1016/j.crv.2010.02.002
- Ward, R. D., Zemlak, T. S., Innes, B. H., Last, P. R., and Hebert, P. D. N. (2005). DNA barcoding Australia's fish species. *Philosophical Transactions of the Royal Society of London. Series B, Biological Sciences* **360**, 1847–1857. doi:10.1098/rstb.2005.1716
- Wiemers, M., and Fiedler, K. (2007). Does the DNA barcoding gap exist? A case study in blue butterflies (Lepidoptera: Lycaenidae). *Frontiers in Zoology* **4**, 8. doi:10.1186/1742-9994-4-8
- Will, K. W., and Rubinoff, D. (2004). Myth of the molecule: DNA barcodes for species cannot replace morphology for identification and classification. *Cladistics* **20**, 47–55. doi:10.1111/j.1096-0031.2003.00008.x
- Zimmer, R. L. (1964). Reproductive biology and development of Phoronida. Ph.D. Thesis, University of Washington, Seattle. [Available from Xerox University Microfilms, Ann Arbor, Michigan.]
- Zhang, A. B., Muster, C., and Liang, H. B. (2012). A fuzzy-set-theory-based approach to analyze species membership in DNA barcoding. *Molecular Ecology* **21**, 1848–1863. doi:10.1111/j.1365-294X.2011.05235.x
- Zhang, J., Kapli, P., Pavlidis, P., and Stamatakis, A. (2013). A general species delimitation method with applications to phylogenetic placements. *Bioinformatics* **29**(22), 2869–2876. doi:10.1093/bioinformatics/btt499

Handling editor: Nerida Wilson